Mathematisches Forschungsinstitut Oberwolfach

Report No. 44/2010

DOI: 10.4171/OWR/2010/44

Mini-Workshop: Shearlets

Organised by
Gitta Kutyniok, Osnabrück
Demetrio Labate, Houston

October 3rd – October 9th, 2010

Abstract. Over the last 20 years, multiscale methods and wavelets have revolutionized the field of applied mathematics by providing an efficient means for encoding isotropic phenomena. Directional multiscale systems, particularly shearlets, are now having the same dramatic impact on the encoding of multivariate signals. Since its introduction about five years ago, the theory of shearlets has rapidly developed and gained wide recognition as the superior way of achieving a truly unified treatment in both the continuum and digital setting. By now, shearlet analysis has reached maturity as a research field, with deep mathematical results, efficient numerical methods, and a variety of high-impact applications. The main goal of the Mini-Workshop *Shearlets* was to gather the world's experts in this field in order to foster closer interaction, attack challenging open problems, and identify future research directions.

Mathematics Subject Classification (2000): 42C15, 42C40.

Introduction by the Organisers
Shearlets: The First Five Years

The Mini-Workshop *Shearlets*, organized by Gitta Kutyniok (Osnabrück) and Demetrio Labate (Houston) was held October 4th–October 8th, 2010. This meeting was attended by 16 participants whose background ranged from the theory of group representations over approximation theory to image analysis. This unique selection provided the ideal setting for a vivid and fertile discussion of the theory and applications of shearlets, a novel multiscale approach particularly designed for multivariate problems.

Multivariate problems in applied mathematics are typically governed by anisotropic phenomena such as singularities concentrated on lower dimensional embedded manifolds or edges in digital images. Wavelets and multiscale methods, which were extensively exploited during the past 25 years for a wide range of both theoretical and applied problems, have been shown to be suboptimal for the encoding of anisotropic features. To overcome these limitations, several intriguing approaches such as ridgelets, contourlets, and curvelets, have since then been proposed, which all provide optimally sparse approximations of anisotropic features. Among those, shearlets are unique in encompassing the mathematical framework of affine systems and are, to date, the only approach capable of achieving a truly unified treatment in both the continuum and digital setting. This includes a precise mathematical analysis of sparse approximation properties in both settings as well as numerically efficient discrete transforms. Therefore shearlets are regarded as having the same potential impact on the encoding of multivariate signals as traditional wavelets did about 20 years ago for univariate problems.

Shearlet systems are designed to efficiently encode anisotropic features such as singularities concentrated on lower dimensional embedded manifolds. To achieve optimal sparsity, shearlets are scaled according to a parabolic scaling law encoded in the *parabolic scaling matrix* A_a, $a > 0$, and exhibit directionality by parameterizing slope encoded in the *shear matrix* S_s, $s \in \mathbb{R}$, defined by

$$A_a = \begin{pmatrix} a & 0 \\ 0 & \sqrt{a} \end{pmatrix} \qquad \text{and} \qquad S_s = \begin{pmatrix} 1 & s \\ 0 & 1 \end{pmatrix},$$

respectively. Hence, shearlet systems are based on three parameters: $a > 0$ being the *scale parameter* measuring the resolution level, $s \in \mathbb{R}$ being the *shear parameter* measuring the directionality, and $t \in \mathbb{R}^2$ being the *translation parameter* measuring the position. This parameter space $\mathbb{R}^+ \times \mathbb{R} \times \mathbb{R}^2$ can be endowed with the group operation

$$(a, s, t) \cdot (a', s', t') = (aa', s + s'\sqrt{a}, t + S_s A_a t'),$$

leading to the so-called *shearlet group* $\mathbb{S}$, which can be regarded as a special case of the general affine group. The *continuous shearlet systems* arise from the unitary group representation

$$\sigma : \mathbb{S} \to \mathcal{U}(L^2(\mathbb{R}^2)), \quad (\sigma(a, s, t)\psi)(x) = a^{-3/4}\psi(A_a^{-1} S_s^{-1}(x - t))$$

and are defined by

$$\{\psi_{a,s,t} = \sigma(a, s, t)\psi = a^{-3/4}\psi(A_a^{-1} S_s^{-1}(\,\cdot\, - t)) : (a, s, t) \in \mathbb{S}\}.$$

For appropriate choices of the *shearlet* $\psi \in L^2(\mathbb{R}^2)$, the *Continuous Shearlet Transform*

$$\mathcal{SH}_\psi : f \to \mathcal{SH}_\psi f(a, s, t) = \langle f, \psi_{ast} \rangle,$$

is a linear isometry from $L^2(\mathbb{R}^2)$ to $L^2(\mathbb{S})$. Alternatively, rather than defining the shearing parameter s on $\mathbb{R}$, the domain can be restricted to, say, $|s| \leq 1$. This gives rise to the so-called *Cone-adapted Continuous Shearlet Transform*, which allows an equal treatment of all directions in contrast to a slightly biased treatment by the Continuous Shearlet Transform. In fact, it could be proven that the Cone-adapted Continuous Shearlet Transform resolves the wavefront set of distributions and can be applied to precisely characterize edges in images. Notice that, although directions are treated slightly biased, the Continuous Shearlet Transform has the

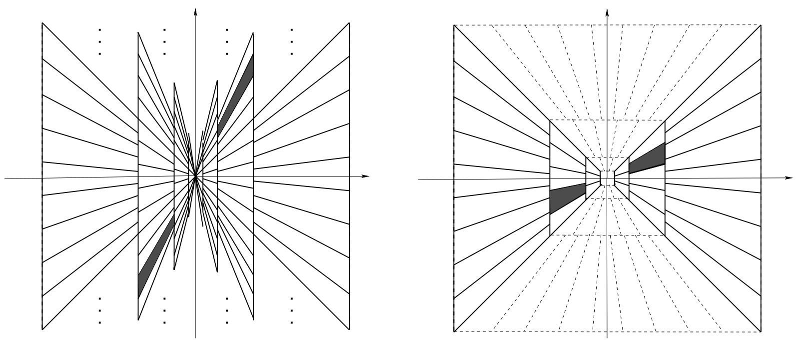

FIGURE 1. Left to Right: Frequency tiling of a discrete shearlet system; Frequency tiling of a cone-adapted discrete shearlet system.

advantage of being equipped with a simpler mathematical structure. This allows the application of group theoretic methodologies to, for instance, discretize the set of parameters through coorbit theory.

Discrete shearlet system are obtained by appropriate sampling of the continuous shearlet systems presented above. Specifically, for $\psi \in L^2(\mathbb{R}^2)$, a *(discrete) shearlet system* is a collection of functions of the form

$$\{\psi_{j,k,m} = 2^{3j/4}\psi(S_k A_{2^j}\ \cdot\ -m) : j \in \mathbb{Z}, k \in K \subset \mathbb{Z}, m \in \mathbb{Z}^2\}, \tag{1}$$

where K is a carefully chosen indexing set of shears. Notice that the shearing matrix S_k maps the digital grid $\mathbb{Z}^2$ onto itself, which is the key idea for deriving a unified treatment of the continuum and digital setting. The discrete shearlet system defines a collection of waveforms at various scales j, orientations controlled by k, and locations dependent on m. In particular, if $K = \mathbb{Z}$ in (1), the shearlet system contains elements oriented along all possible slopes as illustrated in Figure 1. This particular choice is in accordance with the continuous shearlet systems generated by a group action. To avoid the already mentioned biased treatment of directions which the discrete systems inherit, the *cone-adapted discrete shearlet systems* were introduced as

$$\{\phi(\cdot - m) : m \in \mathbb{Z}^2\} \cup \{\psi_{j,k,m}, \tilde{\psi}_{j,k,m} : j \geq 0, |k| \leq \lceil 2^{j/2} \rceil, m \in \mathbb{Z}^2\},$$

where $\tilde{\psi}_{j,k,m}$ is generated from $\psi_{j,k,m}$ by interchanging both variables, and $\psi, \tilde{\psi}$, and ϕ are L^2 functions. Figure 1 illustrates a typical frequency tiling associated with a cone-adapted shearlet system. A suitable choice of the shearlets ψ and $\tilde{\psi}$ generates well-localized shearlet systems which form frames or even Parseval frames.

Over the last years, an abundance of results on the theory and applications of shearlets have been derived by a constantly growing community of researchers. One main goal of this workshop was to discuss the state of the art of this vivid research area. The talks which were delivered by the participants covered the following topics:

(1) *(Cone-adapted) Continuous Shearlet Systems.* Novel results for continuous shearlet systems were presented by S. Dahlke and G. Teschke, who exploited their group structure through a coorbit theory approach to derive feasible discretization of the shearlet parameters as well as associated function spaces even for the 3D setting. F. DeMari's talk then revealed intriguing properties of the set of groups the shearlet group belongs to. Focusing on cone-adapted continuous shearlet systems instead, the microlocal properties of such systems were presented by P. Grohs, and their application to the characterization of edges for 2D and 3D data was discussed by K. Guo.

(2) *(Cone-adapted) Discrete Shearlet Systems.* Recently, compactly supported discrete shearlet systems which provide optimally sparse approximations of anisotropic features were introduced for both 2D and 3D signals to allow superior spatial localization. These novel results were presented by J. Lemvig and W. Lim.

(3) *Numerical Implementations and Applications.* Different efficient numerical implementations of the shearlet transform have been proposed in the past, but further improvements are desirable to achieve additional computational efficiency and features such as locality. W. Lim presented a new fast shearlet transform in his talk which is extremely competitive for applications such as denoising and data separation. A subdivision approach towards a shearlet multiresolution analysis with associated fast decomposition algorithm was discussed by T. Sauer. G. Easley and V. Patel then showed that the shearlet approach is extremely competitive in a wide range of applications from signal and image processing including edge detection, halftoning and image deconvolution.

A further main objective of the workshop was to foster interaction in order to attack a number of open problems and identify future directions of this area of research. During our discussions, the following topics and problems have emerged as main themes to be investigated within the next five years:

- *Shearlet Smoothness Spaces.* For problems arising in the theory of partial differential equations and in approximation theory, it is essential to precisely understand the nature of the spaces defined using shearlets as building blocks and their relation to classical function spaces.
- *Shearlet Constructions and Applications in 3D.* While the theory of shearlets is well understood in the bivariate case, the extension to higher dimensions is still far from being complete. Open problems in this direction include, in particular, the analysis of corner and irregular surface points using shearlets.
- *Construction of "good" Shearlet Systems.* Several results are known, by now, for compactly supported shearlet systems, which though do not form

tight frames. Thus, it would be highly desirable to construct well localized shearlet systems which are compactly supported, form a tight frame or even an orthonormal system, and provide provably optimal sparse approximations of anisotropic features.

- *Numerical Implementations.* Starting with the bivariate situation, one main goal is to derive a complete analog of the fast wavelet transform in the sense of a fast algorithm with associated multiresolution structure paralleling the continuum setting. Furthermore, as the theory for sparse 3D shearlet representations is emerging, numerical implementations for the trivariate case are also in demand. The higher complexity of such data poses a particular difficulty.

The organizers:

G. Kutyniok and D. Labate

Program of the Workshop

Monday, October 4		
09:15–10:00	G. Kutyniok and D. Labate	Opening remarks. Shearlets: the first five years
10:00–10:30	Discussion about the goals of the workshop	
11:00–12:00	P. Grohs	The continuous shearlet transform: reproducing formulae and microlocal analysis
16:00–17:00	S. Dahlke	Shearlet coorbit spaces I: general setting (in arbitrary space dimensions)
17:00–18:00	G. Teshke	Shearlet coorbit Spaces II: compactly supported shearlets, traces and embeddings
Tuesday, October 5		
09:15–10:15	K. Guo	Optimally sparse representations of 3D data using Parseval frames of shearlets
10:15–11:15	W. Lim	Construction and applications of compactly supported shearlets
11:30–12:30	J. Lemvig	Optimally sparse approximations of functions in $L^2(R^3)$ with piecewise C^2 singularities using shearlets
16:00–17:00	F. De Mari	An introduction to mocklets
17:00–18:00	Discussion on continuous shearlets	
Wednesday, October 6		
09:15–10:15	T. Sauer	Shearlet multiresolution and adaptive directional multiresolution.
10:15–10:50	G. Easley	Image processing applications using shearlets
10:50–11:30	V. Patel	Image restoration and enhancement using shearlets
11:30–12:30	Discussion on discrete shearlets	
Thursday, October 7		
09:15–10:15	G. Steidl	Structure tensors and relatives in image processing.
10:15–11:15	X. Zhuang	Interpolating refinable function vectors and matrix extension with symmetry
11:45–12:30	Group discussions	
16:00–18:30	Group discussions	
Friday, October 8		
9:15–10:15	Discussion on future directions	
10:30–12:30	Group discussions	

Mini-Workshop: Shearlets

Table of Contents

Abstracts

The Continuous Shearlet Transform: Representation Formulae and Microlocal Analysis

Philipp Grohs

1. Introduction

In this talk we considered two aspects of the continuous shearlet transform: Representation formulae and the ability of of the shearlet transform to characterize microlocal smoothness properties of bivariate functions.

We start with some notation: Let $D_M : f(x) \mapsto |\det(M)|^{-1/2} f(M^{-1}x), x \in \mathbb{R}^2$ be a matrix dilation operator and $U_s = \begin{pmatrix} 1 & s \\ 0 & 1 \end{pmatrix}$, $W_a = \begin{pmatrix} a & 0 \\ 0 & a^{1/2} \end{pmatrix}$ be shear and anisotropic dilation matrices. Then the shearlet transform of a bivariate function f with respect to a shearlet generator ψ is defined via

$$(a,s,t) \to \mathcal{SH}_\psi f(a,s,t) := \langle f, T_t D_{U_s} D_{W_a} \psi \rangle, \quad (a,s,t) \in \mathbb{R}_+ \times \mathbb{R} \times \mathbb{R}^2$$

where $\psi_{ast} = T_t D_{U_s} D_{W_a} \psi$. The parameters (a,s,t) encode scale, direction and location, respectively. It is easily seen that the distribution of the directions becomes less uniform as s becomes large. This has led to the development of the *cone-adapted shearlet transform* [4]. The idea is to decompose f into $f = P_\mathcal{C} f + P_{\mathcal{C}^\nu} f$, where $P_\mathcal{C}, P_{\mathcal{C}^\nu}$ denote frequency projections onto the cone with slope ≤ 1, resp. ≥ 1. This way it is possible to restrict the shear parameter to a compact set and thus to produce a near uniform sampling of the directions.

2. Representation Formulae

The starting point of our work is [5], where it is shown that with bandlimited shearlet generators, defined by $\hat{\psi}(\xi_1,\xi_2) := \hat{\psi}_1(\xi_1)\hat{\psi}_2(\xi_2/\xi_1)$, $\hat{\psi}^\nu(\xi_1,\xi_1) = \hat{\psi}(\xi_2,\xi_1)$, supp $\hat{\psi}_1 \subset [-2,-1/2] \cup [1/2,2]$, supp $\hat{\psi}_2 \subset [-1,1]$ there holds a representation formula

$$f(x) = \int_{t\in\mathbb{R}^2} \langle f, T_t W \rangle T_t W(x) dt + \int_{\mathbb{R}^2} \int_{-2}^{2} \int_0^1 \mathcal{SH}_\psi P_\mathcal{C} f(a,s,t) P_\mathcal{C} \psi_{ast}(x) \frac{da}{a^3} ds dt$$
$$\int_{\mathbb{R}^2} \int_{-2}^{2} \int_0^1 \mathcal{SH}_{\psi^\nu} P_{\mathcal{C}^\nu} f(a,s,t) P_{\mathcal{C}^\nu} \psi^\nu_{ast}(x) \frac{da}{a^3} ds dt$$

with W an appropriate low-pass function. The main drawback of this formula is its lack of locality. First, the fact that the generators ψ, ψ^ν are bandlimited forces them to be non compactly supported. Second, the operators $P_\mathcal{C}$, $P_{\mathcal{C}^\nu}$ are highly nonlocal. It turns out that the first problem can be dealt with, but one cannot dispense of some sort of frequency localization onto the cones:

Theorem 1 [2]**.** *Under reasonable assumptions (spacial decay, smoothness, vanishing moments) on ψ there does not exist a representation formula*

$$f(x) = C\left(\int_{t\in\mathbb{R}^2} \langle f, T_t W\rangle T_t W(x) dt + \int_{\mathbb{R}^2}\int_{-2}^{2}\int_0^1 \mathcal{SH}_\psi f(a,s,t)\psi_{ast}(x)\frac{da}{a^3} dsdt \right.$$
$$\left. \int_{\mathbb{R}^2}\int_{-2}^{2}\int_0^1 \mathcal{SH}_\psi f(a,s,t)\psi^\nu_{ast}(x)\frac{da}{a^3} dsdt\right)$$

with W smooth.

What we *can* do is to 'localize' the frequency projections and then we obtain the following result:

Theorem 2 [2]**.** *Under reasonable assumptions (spacial decay, smoothness, vanishing moments) on ψ there exist a constant C, compactly supported tempered distributions q, q^ν and a smooth function W so that*

$$f(x) = C\left(\int_{t\in\mathbb{R}^2} \langle f, T_t W\rangle T_t W(x) dt + \int_{\mathbb{R}^2}\int_{-2}^{2}\int_0^1 \mathcal{SH}_\psi f(a,s,t) q * \psi_{ast}(x)\frac{da}{a^3} dsdt \right.$$
$$\left. \int_{\mathbb{R}^2}\int_{-2}^{2}\int_0^1 \mathcal{SH}_\psi f(a,s,t) q^\nu * \psi^\nu_{ast}(x)\frac{da}{a^3} dsdt\right)$$

3. Microlocal Analysis

Shearlets are well-suited for the characterization of microlocal smoothness properties of bivariate tempered distributions. In [5] it is shown that the decay rate of the shearlet coefficients of f with bandlimited generators exactly determines the wavefront set of f. Intuitively, the wavefront set consists of the point-direction pairs where f is not smooth, see [1, 5] for the precise definition. In [3] we show that the assumptions on the generators ψ can be relaxed to non-bandlimited generators with directional vanishing moments.

A finer notion of microlocal smoothness is described by microlocal Sobolev spaces. We say that $f \in W_2^\alpha(t_0, s_0)$ iff there exists a bump function Φ around t_0 such that the frequency projection of Φf onto a cone around the direction associated with s_0 lies in the usual Sobolev space W_2^α, see [1] for the precise definition. We have the following result:

Theorem 3. *$f \in L_2$ is in $W_2^\alpha(t_0, s_0)$ if and only if there exists a neighborhood U of t_0 and V of s_0 such that*

$$S^\alpha(t,s) \in L_2\left(U \times V, dtds\right)$$

and

$$S^\alpha(t,s) := \left(\int_0^1 |\mathcal{SH}_\psi f(a,s,t) a^{-\alpha}|^2 \frac{da}{a^3}\right)^{1/2},$$

provided that ψ has sufficiently many vanishing moments and is sufficiently smooth.

References

[1] E. Candes and D. Donoho, *The Continuous Curvelet Transform I: Resolution of the Wavefront Set*, Applied and Computational Harmonic Analysis **19** (2003), 162–197.
[2] P. Grohs, *Continuous Shearlet Tight Frames*, Journal of Fourier Analysis and Applications (2010), to appear.
[3] P. Grohs, *Continuous Shearlet Frames and Resolution of the Wavefront Set*, Monatshefte für Mathematik (2010), submitted.
[4] K. Guo, G. Kutyniok and D. Labate, *Sparse Multidimensional Representations using Anisotropic Dilation and Shear Operators*, Wavelets and Splines (Athens, GA, 2005), Nashboro Press, Nashville, TN (2006), 189-201.
[5] G. Kutyniok and D. Labate, *Resolution of the Wavefront Set using Continuous Shearlets*, Transactions of the AMS **361** (2009), 2719–2754.

Shearlet coorbit spaces I: General setting (in arbitrary space dimensions)

Stephan Dahlke

(joint work with Gabriele Steidl, Gerd Teschke)

Multivariate Continuous Shearlet Transform. Let us start by introducing the continuous shearlet transform on $L_2(\mathbb{R}^n)$. This requires the generalization of the parabolic dilation matrix and of the shear matrix. Let I_n denote the (n,n)-identity matrix and 0_n, resp. 1_n the vectors with n entries 0, resp. 1. For $a \in \mathbb{R}^* := \mathbb{R} \setminus \{0\}$ and $s \in \mathbb{R}^{n-1}$, we set

$$A_a := \begin{pmatrix} a & 0_{n-1}^{\mathrm{T}} \\ 0_{n-1} & \operatorname{sgn}(a)|a|^{\frac{1}{n}}\, I_{n-1} \end{pmatrix} \quad \text{and} \quad S_s := \begin{pmatrix} 1 & s^{\mathrm{T}} \\ 0_{n-1} & I_{n-1} \end{pmatrix}.$$

Lemma 1. *The set $\mathbb{R}^* \times \mathbb{R}^{n-1} \times \mathbb{R}^n$ endowed with the operation*

$$(a,s,t) \circ (a',s',t') = (aa', s + |a|^{1-1/n}\, s', t + S_s A_a t')$$

is a locally compact group $\mathbb{S}$ which we call full shearlet group*. The left and right Haar measures on $\mathbb{S}$ are given by*

$$d\mu_l(a,s,t) = \frac{1}{|a|^{n+1}}\, da\, ds\, dt \quad \text{and} \quad d\mu_r(a,s,t) = \frac{1}{|a|}\, da\, ds\, dt.$$

For $f \in L_2(\mathbb{R}^n)$ we define

$$\pi(a,s,t)f(x) = f_{a,s,t}(x) := |a|^{\frac{1}{2n}-1} f(A_a^{-1} S_s^{-1}(x-t)). \tag{1}$$

Theorem 2. *The mapping π defined by (1) is a unitary representation of $\mathbb{S}$. Moreover, a function $\psi \in L_2(\mathbb{R}^n)$ is admissible if and only if*

$$C_\psi := \int_{\mathbb{R}^n} \frac{|\hat{\psi}(\omega)|^2}{|\omega_1|^n}\, d\omega < \infty. \tag{2}$$

Then, for any $f \in L_2(\mathbb{R}^n)$, the following equality holds true:

$$\int_{\mathbb{S}} |\langle f, \psi_{a,s,t}\rangle|^2 \, d\mu_l(a,s,t) = C_\psi \, \|f\|^2_{L_2(\mathbb{R}^n)}. \tag{3}$$

Multivariate Shearlet Coorbit Theory. We consider weight functions $w(a,s,t) = w(a,s)$ that are locally integrable with respect to a and s, i.e., $w \in L_1^{loc}(\mathbb{R}^n)$ and fulfill $w\left((a,s,t) \circ (a',s',t')\right) \leq w(a,s,t)w(a',s',t')$ and $w(a,s,t) \geq 1$. Let

$$L_{p,w}(\mathbb{S}) := \{F \; : \|F\|_{L_{p,w}(\mathbb{S})} := \left(\int_{\mathbb{S}} |F(g)|^p \, w(a,s,t)^p d\mu(a,s,t)\right)^{1/p} < \infty\}.$$

In order to construct the coorbit spaces related to the shearlet group we have to ensure that there exists a function $\psi \in L_2(\mathbb{R}^n)$ such that

$$\mathcal{SH}_\psi(\psi) = \langle \psi, \pi(a,s,t)\psi\rangle \in L_{1,w}(\mathbb{S}). \tag{4}$$

Theorem 3. *Let ψ be a Schwartz function such that* $\operatorname{supp}\hat{\psi} \subseteq ([-a_1,-a_0] \cup [a_0,a_1]) \times [-b_1,b_1] \times \cdots \times [-b_{n-1},b_{n-1}]$. *Then we have that* $\mathcal{SH}_\psi(\psi) \in L_{1,w}(\mathbb{S})$.
For ψ satisfying (4) we can consider the space

$$\mathcal{H}_{1,w} := \{f \in L_2(\mathbb{R}^n) : \mathcal{SH}_\psi(f) = \langle f, \pi(\cdot)\psi\rangle \in L_{1,w}(\mathbb{S})\}, \tag{5}$$

with norm $\|f\|_{\mathcal{H}_{1,w}} := \|\mathcal{SH}_\psi f\|_{L_{1,w}(\mathbb{S})}$ and its anti-dual $\mathcal{H}_{1,w}^{\sim}$. The spaces $\mathcal{H}_{1,w}$ and $\mathcal{H}_{1,w}^{\sim}$ are π-invariant Banach spaces with continuous embeddings $\mathcal{H}_{1,w} \hookrightarrow \mathcal{H} \hookrightarrow \mathcal{H}_{1,w}^{\sim}$, and their definition is independent of the shearlet ψ. Then the inner product on $L_2(\mathbb{R}^n) \times L_2(\mathbb{R}^n)$ extends to a sesquilinear form on $\mathcal{H}_{1,w}^{\sim} \times \mathcal{H}_{1,w}$, therefore for $\psi \in \mathcal{H}_{1,w}$ and $f \in \mathcal{H}_{1,w}^{\sim}$ the *extended representation coefficients*

$$\mathcal{SH}_\psi(f)(a,s,t) := \langle f, \pi(a,s,t)\psi\rangle_{\mathcal{H}_{1,w}^{\sim} \times \mathcal{H}_{1,w}}$$

are well-defined. The next step is to consider an additional weight function m which is *moderate* with respect to w, i.e., $m((a,s,t) \circ (a',s',t') \circ (a'',s'',t'')) \leq w(a,s,t)m(a',s',t')w(a'',s'',t'')$. Then, with respect to the new weight m, we define the *shearlet coorbit spaces*

$$\mathcal{SC}_{p,m} := \{f \in \mathcal{H}_{1,w}^{\sim} : \mathcal{SH}_\psi(f) \in L_{p,m}(\mathbb{S})\} \tag{6}$$

with norms $\|f\|_{\mathcal{SC}_{p,m}} := \|\mathcal{SH}_\psi f\|_{L_{p,m}(\mathbb{S})}$.

The Feichtinger-Gröchenig theory provides us with a machinery to construct atomic decompositions and Banach frames for our shearlet coorbit spaces $\mathcal{SC}_{p,w}$. A (countable) family $X = ((a,s,t)_\lambda)_{\lambda\in\Lambda}$ in $\mathbb{S}$ is said to be *U-dense* if $\cup_{\lambda\in\Lambda}(a,s,t)_\lambda U = \mathbb{S}$, and *separated* if for some compact neighborhood Q of e we have $(a_i,s_i,t_i)Q \cap (a_j,s_j,t_j)Q = \emptyset, i \neq j$, and *relatively separated* if X is a finite union of separated sets.

Lemma 4. *Let U be a neighborhood of the identity in $\mathbb{S}$, and let $\alpha > 1$ and $\beta, \gamma > 0$ be defined such that $[\alpha^{\frac{1}{n}-1}, \alpha^{\frac{1}{n}}) \times [-\frac{\beta}{2}, \frac{\beta}{2})^{n-1} \times [-\frac{\gamma}{2}, \frac{\gamma}{2})^n \subseteq U$. Then the sequence*

$$\{(\epsilon\alpha^j, \beta\alpha^{j(1-\frac{1}{n})}k, S_{\beta\alpha^{j(1-\frac{1}{n})}k}A_{\alpha^j}\gamma m) : j \in \mathbb{Z}, k \in \mathbb{Z}^{n-1}, m \in \mathbb{Z}^n, \epsilon \in \{-1,1\}\}$$

is U-dense and relatively separated.

Next we define the *U–oscillation* as

$$\operatorname{osc}_U(a,s,t) := \sup_{u\in U} |\mathcal{SH}_\psi(\psi)(u\circ(a,s,t)) - \mathcal{SH}_\psi(\psi)(a,s,t)|. \tag{7}$$

Then, the following decomposition theorem, which was proved in a general setting in [3, 4, 5], says that discretizing the representation by means of an U-dense set produces an atomic decomposition for $\mathcal{SC}_{p,w}$.

Theorem 5. *Assume that the irreducible, unitary representation π is w-integrable and let an appropriately normalized $\psi \in L_2(\mathbb{R}^n)$ which fulfills*

$$M\langle\psi,\pi(a,s,t)\rangle := \sup_{u\in(a,s,t)U} |\langle\psi,\pi(u)\psi\rangle| \in L_{1,w}(\mathbb{S}) \tag{8}$$

be given. Choose a neighborhood U of e so small that $\|\operatorname{osc}_U\|_{L_{1,w}(\mathbb{S})} < 1$. Then for any U-dense and relatively separated set $X = ((a,s,t)_\lambda)_{\lambda\in\Lambda}$ the space $\mathcal{SC}_{p,m}$ has the following atomic decomposition: *If $f \in \mathcal{SC}_{p,m}$, then*

$$f = \sum_{\lambda\in\Lambda} c_\lambda(f)\pi((a,s,t)_\lambda)\psi \tag{9}$$

where the sequence of coefficients depends linearly on f and satisfies

$$\|(c_\lambda(f))_{\lambda\in\Lambda}\|_{\ell_{p,m}} \sim \|f\|_{\mathcal{SC}_{p,m}}. \tag{10}$$

Given such an atomic decomposition, the problem arises under which conditions a function f is completely determined by its *moments* $\langle f,\pi((a,s,t)_\lambda)\psi\rangle$ and how f can be reconstructed from these moments.

Theorem 6. *Impose the same assumptions as in Theorem 5. Choose a neighborhood U of e such that $\|\operatorname{osc}_U\|_{L_{1,w}(\mathbb{S})} < 1/\|\mathcal{SH}_\psi(\psi)\|_{L_{1,w}(\mathbb{S})}$. Then the set*

$$\{\pi((a,s,t)_\lambda)\psi : \lambda\in\Lambda\}$$

is a Banach frame for $\mathcal{SC}_{p,m}$. This means that

i) *$f \in \mathcal{SC}_{p,m}$ if and only if $(\langle f,\pi((a,s,t)_\lambda)\psi\rangle_{\mathcal{H}^\sim_{1,w}\times\mathcal{H}_{1,w}})_{\lambda\in\Lambda} \in \ell_{p,m}$;*

ii)
$$\|f\|_{\mathcal{SC}_{p,m}} \sim \|(\langle f,\pi((a,s,t)_\lambda)\psi\rangle_{\mathcal{H}^\sim_{1,w}\times\mathcal{H}_{1,w}})_{\lambda\in\Lambda}\|_{\ell_{p,m}};$$

iii) *there exists a bounded, linear operator $\mathcal{S}$ from $\ell_{p,m}$ to $\mathcal{SC}_{p,m}$ such that $\mathcal{S}\left((\langle f,\psi((a,s,t)_\lambda)\psi\rangle_{\mathcal{H}^\sim_{1,w}\times\mathcal{H}_{1,w}})_{\lambda\in\Lambda}\right) = f$.*

To apply the whole machinery it remains to prove that $\|\operatorname{osc}_U\|_{L_{1,w}(\mathbb{S})}$ becomes arbitrarily small for a sufficiently small neighborhood U of e.

Theorem 7. *Let ψ be a function contained in the Schwartz space $\mathcal{S}$ with* $\operatorname{supp}\hat{\psi} \subseteq ([-a_1,-a_0]\cup[a_0,a_1]) \times_b [-b_1,b_1]\times\cdots\times[-b_{n-1},b_{n-1}]$. *Then, for every $\varepsilon > 0$, there exists a sufficiently small neighborhood U of e so that*

$$\|\operatorname{osc}_U\|_{L_{1,w}(\mathbb{S})} \le \varepsilon. \tag{11}$$

Further information concerning the coorbit and group theory related with the continuous shearlet transform can be found in [1, 2].

References

[1] S. Dahlke, G. Kutyniok, G. Steidl, and G. Teschke, *Shearlet coorbit spaces and associated Banach frames*, Appl. Comput. Harmon. Anal. **27/2** (2009), 195–214.

[2] S. Dahlke, G. Steidl, and G. Teschke, *The continuous shearlet transform in arbitrary space simensions* J. Fourier Anal. Appl. **16** (2010), 340-354.

[3] H. G. Feichtinger and K. Gröchenig, *Banach spaces related to integrable group representations and their atomic decomposition I,* J. Funct. Anal. **86** (1989), 307–340.

[4] H. G. Feichtinger and K. Gröchenig, *Banach spaces related to integrable group representations and their atomic decomposition II,* Monatsh. Math. **108** (1989), 129–148.

[5] K. Gröchenig, *Describing functions: Atomic decompositions versus frames,* Monatsh. Math. **112** (1991), 1–42.

Shearlet Coorbit Spaces II: Compactly Supported Shearlets, Traces and Embeddings

Gerd Teschke

(joint work with Stephan Dahlke, Gabriele Steidl)

We show that compactly supported functions with sufficient smoothness and enough vanishing moments can serve as analyzing vectors for shearlet coorbit spaces. We use this approach to prove embedding theorems for subspaces of shearlet coorbit spaces resembling shearlets on the cone into Besov spaces. Furthermore, we show embedding relations of traces of these subspaces with respect to the real axes.

The Shearlet group and the continuous Shearlet transform. The (full) shearlet group SS is defined to be the set $\mathbb{R}^* \times \mathbb{R} \times \mathbb{R}^2$ endowed with the group operation $(a, s, t)\,(a', s', t') = (aa', s+s'\sqrt{|a|}, t+S_s A_a t')$. A right–invariant and left-invariant Haar measures of SS is given by $\mu_{SS,r} = da/|a|\,ds\,dt$ and $\mu_{SS,l} = da/|a|^3\,ds\,dt$, respectively and the modular function of $\mathbb{S}$ by $\triangle(a, s, t) = 1/|a|^2$. For the shearlet group the mapping $\pi : \mathbb{S} \to \mathcal{U}(L_2(\mathbb{R}^2))$ defined by

$$\pi(a, s, t)\,\psi(x) := |a|^{-\frac{3}{4}}\,\psi\left(\frac{1}{a}\,(x_1 - t_1 - s(x_2 - t_2))\,, \frac{\operatorname{sgn} a}{\sqrt{|a|}}\,(x_2 - t_2)\right) \tag{1}$$

is a unitary representation of $\mathbb{S}$, see [1, 2]. With the help of [2] it follows that the unitary representation π defined in (1) is a square-integrable representation of $\mathbb{S}$. The transform $\mathcal{SH}_\psi : L_2(\mathbb{R}^2) \to L_2(\mathbb{S})$ defined by $\mathcal{SH}_\psi f(a, s, t) := \langle f, \psi_{a,s,t}\rangle$ is called Continuous Shearlet Transform.

Shearlet coorbit spaces from Shearlets with compact support. Let w be a positive, real-valued, continuous submultiplicative weight on $\mathbb{S}$. To define our coorbit spaces we need the set $\mathcal{A}_w := \{\psi \in L_2(\mathbb{R}^2) : \mathcal{SH}_\psi(\psi) = \langle \psi, \pi(\cdot)\psi\rangle \in L_{1,w}\}$ of analyzing vectors, see [3, 4, 5, 7]. In the following, we assume that our weight is symmetric with respect to the modular function, i.e., $w(g) = w(g^{-1})\triangle(g^{-1})$. Let $Q_D :=$

$[-D,D]\times[-D,D]$. The following theorem shows that $\mathcal{A}_w$ contains shearlets with compact support.

Theorem 1. *Let $\psi(x)\in L_2(\mathbb{R}^2)$ fulfill* $\operatorname{supp}\psi\in Q_D$. *Suppose that the weight function satisfies $w(a,s,t)=w(a)\le|a|^{-\rho_1}+|a|^{\rho_2}$ for $\rho_1,\rho_2>0$ and that*

$$|\hat{\psi}(\omega_1,\omega_2)|\le C\frac{|\omega_1|^n}{(1+|\omega_1|)^r}\frac{1}{(1+|\omega_2|)^r} \tag{2}$$

with $n\ge\max(\frac{1}{4}+\rho_2,\frac{9}{4}+\rho_1)$ and $r>n+\max(\frac{7}{4}+\rho_2,\frac{9}{4}+\rho_1)$. Then we have that $\mathcal{SH}_\psi(\psi)\in L_{1,w}(\mathbb{S})$.

For an analyzing ψ we can consider

$$\mathcal{H}_{1,w}:=\{f\in L_2(\mathbb{R}^2):\mathcal{SH}_\psi(f)=\langle f,\pi(\cdot)\psi\rangle\in L_{1,w}(\mathbb{S})\}$$

with norm $\|f\|_{\mathcal{H}_{1,w}}:=\|\mathcal{SH}_\psi f\|_{L_{1,w}(\mathbb{S})}$ and its anti-dual $\mathcal{H}_{1,w}^{\sim}$. As the inner product on $L_2(\mathbb{R}^2)\times L_2(\mathbb{R}^2)$ extends to a sesquilinear form on $\mathcal{H}_{1,w}^{\sim}\times\mathcal{H}_{1,w}$, the extended representation coefficients $\mathcal{SH}_\psi(f)(a,s,t):=\langle f,\pi(a,s,t)\psi\rangle_{\mathcal{H}_{1,w}^{\sim}\times\mathcal{H}_{1,w}}$ are well-defined. Let m be a w-moderate weight on $\mathbb{S}$, i.e. $m(xyz)\le w(x)m(y)w(z)$ for all $x,y,z\in\mathbb{S}$. Then we can define the called shearlet coorbit spaces

$$\mathcal{SC}_{p,m}:=\{f\in\mathcal{H}_{1,w}^{\sim}:\mathcal{SH}_\psi(f)\in L_{p,m}(\mathbb{S})\},\quad \|f\|_{\mathcal{SC}_{p,m}}:=\|\mathcal{SH}_\psi f\|_{L_{p,m}(\mathbb{S})}. \tag{3}$$

Atomic decompositions and Shearlet Banach frames. To construct atomic decompositions and Banach frames the subset $\mathcal{B}_w$ of $\mathcal{A}_w$,

$$\mathcal{B}_w:=\{\psi\in L_2(\mathbb{R}^2):\mathcal{SH}_\psi(\psi)\in\mathcal{W}(C_0,L_{1,w})\}$$

has to be non-empty. Here $\mathcal{W}(C_0,L_{1,w}):=\{F:\|(L_x\chi_{\mathcal{Q}})F\|_\infty\in L_{1,w}\}$ and $\mathcal{Q}$ is a relatively compact neighborhood of the identity element in $\mathbb{S}$, see [7]. It can be shown, for a classes of weights w sufficiently smooth and compactly supported $\psi(x)\in L_2(\mathbb{R}^2)$ belong to $\mathcal{B}_w$. As it was shown in [2] that for $\alpha>1$ and $\sigma,\tau>0$ the set $X:=\{(\epsilon\alpha^{-j},\sigma\alpha^{-j/2}k,S_{\sigma\alpha^{-j/2}k}A_{\alpha^{-j}}\tau l):j\in\mathbb{Z},k\in\mathbb{Z},l\in\mathbb{Z}^2,\,\epsilon\in\{-1,1\}\}$ forms a U-dense and relatively separated family, we can deduce by Theorem 3.1 and 3.2 in [2] that we can establish atomic decompositions and Banach frames for the shearlet coorbit spaces.

Structure of Shearlet Coorbit Spaces. We now establish relations between scales of Shearlet coorbit spaces and relations to Besov spaces. To establish relations to Besov spaces we apply the characterization of homogeneous Besov spaces $B^\sigma_{p,q}$ from [6], see also [8, 10]. For inhomogeneous Besov spaces we refer to [9]. The full analysis is restricted to weights $m(a,s,t)=m(a):=|a|^{-r},r\ge 0$, suggesting to use the abbreviation $\mathcal{SC}_{p,r}:=\mathcal{SC}_{p,m}$. For simplicity, we further assume that we can use $\sigma=\tau=1$ in the U-dense, relatively separated set X and restrict ourselves to the case $\epsilon=1$. Therefore, we assume that $f\in\mathcal{SC}_{p,r}$ can be written as

$$f(x)\;=\;\sum_{j\in\mathbb{Z}}\sum_{k\in\mathbb{Z}}\sum_{l\in\mathbb{Z}^2}c(j,k,l)\alpha^{\frac{3}{4}j}\psi(\alpha^jx_1-\alpha^{j/2}kx_2-l_1,\alpha^{j/2}x_2-l_2). \tag{4}$$

To derive reasonable trace and embedding theorems, it is necessary to introduce the following subspaces of $\mathcal{SC}_{p,r}$. For fixed $\psi\in B_w$ we denote by $\mathcal{SCC}_{p,r}$ be the closed subspace of $\mathcal{SC}_{p,r}$ consisting of those functions which are representable as in (4) but with integers $|k| \leq \alpha^{j/2}$. As we shall see in the sequel for each of these ψ the resulting spaces $\mathcal{SCC}_{p,r}$ embed in the same scale of Besov spaces, and the same holds true for the trace theorems.

In most of the classical smoothness spaces like Sobolev and Besov spaces dense subsets of 'nice' functions can be identified.

Theorem 2. *Let* $\mathcal{S}_0 := \{f \in \mathcal{S} : |\hat{f}(\omega)| \leq \omega_1^{2\alpha}(1+\|\omega\|^2)^{-2\alpha} \ \forall \ \alpha > 0\}$ *and* $m(a,s,t) = m(a,s) := |a|^r(1/|a|+|a|+|s|)^n$ *for some* $r \in \mathbb{R}, n \geq 0$. *Then the set of Schwartz functions forms a dense subset of the shearlet coorbit space* $\mathcal{SC}_{p,m}$.

We now investigate the traces of functions lying in $\mathcal{SCC}_{p,r}$ with respect to the horizontal and vertical axes, respectively.

Theorem 3. *Let* $Tr_h f$ *denote the restriction of* f *to the (horizontal)* x_1*-axis, i.e.,* $(Tr_h f)(x_1) := f(x_1, 0)$. *Then* $Tr_h(\mathcal{SCC}_{p,r}) \subset B^{\sigma_1}_{p,p}(\mathbb{R}) + B^{\sigma_2}_{p,p}(\mathbb{R})$, *where*

$$B^{\sigma_1}_{p,p}(\mathbb{R}) + B^{\sigma_2}_{p,p}(\mathbb{R}) := \{h \mid h = h_1 + h_2, h_1 \in B^{\sigma_1}_{p,p}(\mathbb{R}), h_2 \in B^{\sigma_2}_{p,p}(\mathbb{R})\}$$

and the parameters σ_1 *and* σ_2 *satisfy the conditions* $\sigma_1 = r - \frac{5}{4} + \frac{3}{2p}$, $\sigma_2 = r - \frac{3}{4} + \frac{1}{p}$.

Corollary 4. *For* $p = 1$, *the embedding* $Tr_h(\mathcal{SC}_{1,r}) \subset B^{\sigma}_{1,1}(\mathbb{R})$ *with* $\sigma = r - \frac{3}{4} + \frac{1}{p}$ *holds true.*

Theorem 5. *Let* $Tr_v f$ *denote the restriction of* f *to the (vertical)* x_2*-axis, i.e.,* $(Tr_v f)(x_2) := f(0, x_2)$. *Then the embedding* $Tr_v(\mathcal{SCC}_{p,r}) \subset B^{\sigma_1}_{p,p}(\mathbb{R}) + B^{\sigma_2}_{p,p}(\mathbb{R})$, *holds true, where* σ_1 *is the largest number such that* $\sigma_1 + \lfloor \sigma_1 \rfloor \leq 2r - \frac{9}{2} + \frac{3}{p}$, *and* $\sigma_2 = 2r - \frac{3}{2} + \frac{1}{p}$.

We turn now to embedding results.

Corollary 6. *For* $1 \leq p_1 \leq p_2 \leq \infty$ *the embedding* $\mathcal{SC}_{p_1,r} \subset \mathcal{SC}_{p_2,r}$ *holds true. Introducing the 'smoothness spaces'* $\mathcal{G}^r_p := \mathcal{SC}_{p,r+d(\frac{1}{2}-\frac{1}{p})}$. *This implies the continuous embedding* $\mathcal{G}^{r_1}_{p_1} \subset \mathcal{G}^{r_2}_{p_2}$, *if* $r_1 - \frac{d}{p_1} = r_2 - \frac{d}{p_2}$.

Theorem 7. *The embedding* $\mathcal{SCC}_{p,r} \subset B^{\sigma_1}_{p,p}(\mathbb{R}^2) + B^{\sigma_2}_{p,p}(\mathbb{R}^2)$, *holds true, where* σ_1 *is the largest number such that* $\sigma_1 + \lfloor \sigma_1 \rfloor \leq 2r - \frac{9}{2} + \frac{4}{p}$, *and* $\sigma_2 - \frac{\lfloor \sigma_2 \rfloor}{2} = r + \frac{3}{2p} + \frac{1}{4}$.

References

[1] S. Dahlke, G. Kutyniok, P. Maass, C. Sagiv, H.-G. Stark, and G. Teschke, The uncertainty principle associated with the continuous shearlet transform, Int. J. Wavelets Multiresolut. Inf. Process., 6, 157 - 181 (2008).

[2] S. Dahlke, G. Kutyniok, G. Steidl, and G. Teschke, Shearlet coorbit spaces and associated Banach frames, Appl. Comput. Harmon. Anal. 27/2, 195 - 214 (2009).

[3] H. G. Feichtinger and K. Gröchenig, *A unified approach to atomic decompositions via integrable group representations*, Proc. Conf. "Function Spaces and Applications", Lund 1986, Lecture Notes in Math. **1302** (1988), 52 - 73.

[4] H. G. Feichtinger and K. Gröchenig, *Banach spaces related to integrable group representations and their atomic decomposition I,* J. Funct. Anal. **86**, 307 - 340 (1989).

[5] H. G. Feichtinger and K. Gröchenig, *Banach spaces related to integrable group representations and their atomic decomposition II,* Monatsh. Math. **108**, 129 - 148 (1989).

[6] M. Frazier and B. Jawerth, Decomposition of Besov sapces, Indiana University Mathematics Journal **34/4**, 777 - 799 (1985).

[7] K. Gröchenig, *Describing functions: Atomic decompositions versus frames,* Monatsh. Math. **112**, 1 - 42 (1991).

[8] L.I. Hedberg and Y. Netrusov, An axiomatic approach to function spaces, spectral synthesis, and Luzin approximation, Memoirs of the American Math. Soc. **188**, 1- 97 (2007).
[9] C. Schneider, Besov spaces of positive smoothness, PhD thesis, University of Leipzig, 2009.
[10] H. Triebel, Function Spaces I, Birkhäuser, Basel - Boston - Berlin, 2006

Optimally Sparse Representations of 3D Data using Parseval Frames of Shearlets

Kanghui Guo
(joint work with Demetrio Labate)

In a seminal paper from 2004 [1], Candès and Donoho proved a remarkable result about representations of 2-dimensional data, showing that the curvelet representation, a multiscale system of waveforms defined at various directions and positions at each scale, is essentially as good as an adaptive representation from the point of view of its ability to approximate images containing edges. Specifically, for functions f which are C^2 away from C^2 edges, the N term approximation f_N^C obtained from the N largest coefficients of its curvelet expansion, obeys

$$||f - f_N^C||_2^2 \asymp N^{-2}(\log N)^3, \qquad \text{as } N \to \infty. \tag{1}$$

Ignoring the loglike factor, this is the optimal approximation rate for this class of functions while, in comparison, the wavelet and Fourier representations only achieve approximation rate N^{-1} and $N^{-1/2}$, respectively.

The importance of this result goes beyond basic fundamental theoretical questions about the mathematical representations of functions containing edge discontinuities, and has great relevance for a variety of technologies and applications. In fact, the notion of sparsity entails the intimate understanding of the most essential information contained in data, which is critically important for the development of improved algorithms in areas such as data modeling, feature extraction, image denoising and classification.

The *shearlet representation* was introduced by the authors of this paper and their collaborators in [7, 4] as an alternative approach which satisfies the same (essentially) optimally sparse approximation rate (Refeq.opt) when dealing with the same class of 2–D data [5]. However, unlike curvelets, the shearlet approach relies on a simpler mathematical construction, based on the framework of affine systems, so that all elements of the representation system are derived from a single (or finite set of) generators through the action of the affine group. The unique properties of the shearlet approach provide not only the benefit of greater flexibility and mathematical simplicity, but also ensure that there is a natural transition from the continuum to the discrete setting. This was exploited in a wide range of very powerful applications (e.g., [2, 3, 8, 9]).

In particular, the shearlet approach extends naturally to the 3-dimensional setting where it also provides optimally sparse nonadaptive representations of 3–D data. In fact, we can construct a Parseval frame of shearlets to represent 3-dimensional functions f which are smooth away from discontinuities along C^2

boundaries, and prove that the N-term approximation f_N^S, obtained from the N largest coefficients of its shearlet representation, satisfies the estimate:

$$||f - f_N^S||_2^2 \asymp N^{-1}(\log N)^2, \qquad \text{as } N \to \infty. \tag{2}$$

Up the logarithmic factor, this is the optimal approximation rate for this type of function in the sense that no orthonormal bases or Parseval frames can yield approximation rates that are better than N^{-1}. Even if one considers finite linear combinations of elements taken from arbitrary dictionaries, there is no depth-limited search dictionary that can achieve a rate better than N^{-1}. In contrast, more traditional methods based on wavelet and Fourier approximations are significantly less efficient since their asymptotic approximation rate only decays as $N^{-1/2}$ and $N^{-1/3}$, respectively. Notice that this result, recently appeared in [6], is the first and (so far) only published result concerning a nonadaptive construction which is provably optimal (up to a loglike factor) for a large class of 3–D data.

A simple heuristic argument can be used to justify why 3–D shearlet system is optimally efficient when dealing with 3–D data f containing discontinuous surfaces, whereas a 3–D wavelet system cannot be very sparse. Indeed, at scale 2^{-2j}, a wavelet $\phi_{j,k}(x) = 2^{3j}\phi(2^{2j}x - k)$ is essentially supported on a box of size $2^{-2j} \times 2^{-2j} \times 2^{-2j}$. Hence, there are approximately $O(2^{4j})$ wavelet coefficients $C_{j,k}(f) = \langle f, \phi_{j,k} Rangle$ associated with the surface of discontinuity (while the remaining coefficients are negligible at fine scales). Since

$$\int_{\mathbb{R}^3} |\phi_{j,k}(x)|\, dx = 2^{3j} \int_{\mathbb{R}^3} |\phi(2^{2j}x - k)|\, dx = 2^{-3j} \int_{\mathbb{R}^3} |\phi(y)|\, dy,$$

a direct computation shows that, at scale 2^{-2j}, all these wavelet coefficients are controlled by

$$|C_{j,k}(f)| \le ||f||_\infty \, ||\phi_{j,k}||_{L^1} \le C\, 2^{-3j}.$$

If follows that the N-th largest wavelet coefficient $|C_N(f)|$ is bounded by $O(N^{-3/4})$ and, thus, if f_N^W is the approximation of f obtained by taking the N largest coefficients of its wavelet expansion, the L^2–error obeys the estimate:

$$||f - f_N^W||_{L^2}^2 \le \sum_{\ell > N} |C_\ell(f)|^2 \le C\, N^{-1/2}.$$

By contrast, the elements of the shearlet system, denoted by $\psi_{j,\ell,k}$, at scale 2^{-2j}, are essentially supported on a parallelepiped of size $2^{-2j} \times 2^{-j} \times 2^{-j}$, with location controlled by k, and orientation controlled by ℓ. At fine scales (j "large"), it is reasonable to assume that the only significant shearlet coefficients $S_{j,\ell,k}(f) = \langle f, \psi_{j,\ell,k}, Rangle$ are those corresponding to the shearlet elements which are tangent to the surface of discontinuity; there are about $O(2^{2j})$ coefficients of this type. Again, a direct computation shows that

$$\int_{\mathbb{R}^3} |\psi_{j,\ell,k}(x)|\, dx = 2^{-2j} \int_{\mathbb{R}^3} |\psi(y)|\, dy,$$

so that, at scale 2^{-2j}, all these shearlet coefficients are controlled by

$$|S_{j,\ell k}(f)| \le ||f||_\infty \, ||\psi_{j,\ell,k}||_{L^1} \le C\, 2^{-2j}.$$

It follows that the N-th largest shearlet coefficient $|S_N(f)|$ is bounded by $O(N^{-1})$ and this implies that – denoting by f_N is the approximation of f computed by taking the N largest coefficients of its shearlets expansion – the L^2–error approximately obeys the estimate:

$$||f - f_N^S||_{L^2}^2 \leq \sum_{\ell > N} |S_\ell(f)|^2 \leq C\, N^{-1}.$$

The rigorous proof of this result requires a much more sophisticated argument based on techniques from the theory of oscillatory integrals. In particular, the main technical arguments needed to estimate the effect of the surface discontinuities in the shearlet representation require the introduction of a fundamentally new approach which is significantly different from the 2–D case.

References

[1] E. J. Candès and D. L. Donoho, *New tight frames of curvelets and optimal representations of objects with C^2 singularities*, Comm. Pure Appl. Math., **57** (2004), 219–266.

[2] F. Colonna, G. Easley, K. Guo, and D. Labate, *Radon Transform Inversion using the Shearlet Representation*, Appl. Comput. Harmon. Anal. **29**(2)2 (2010), 232–250.

[3] G. R. Easley, D. Labate, F. Colonna, *Shearlet-Based Total Variation Diffusion for Denoising*, IEEE Trans. Image Proc. **18** (2) (2009), 260–268.

[4] K. Guo, G. Kutyniok, and D. Labate, *Sparse Multidimensional Representations using Anisotropic Dilation and Shear Operators,* in: Wavelets and Splines, G. Chen and M. Lai (eds.), Nashboro Press, Nashville, TN (2006), pp. 189–201.

[5] K. Guo, D. Labate, *Optimally Sparse Multidimensional Representation using Shearlets*, SIAM J. Math. Anal., **9** (2007), 298–318

[6] K. Guo, D. Labate, *Optimally Sparse 3–D Approximations using Shearlet Representations*, Electron. Res. Announc. Math. Sci., **17** (2010), 126–138

[7] K. Guo, W.-Q Lim, D. Labate, G. Weiss and E. Wilson, *Wavelets with composite dilations*, Electron. Res. Announc. Amer. Math. Soc., **10** (2004), 78–87

[8] G. Kutyniok and T. Sauer. *Adaptive Directional Subdivision Schemes and Shearlet Multiresolution Analysis*, SIAM J. Math. Anal. **41** (2009), 1436–1471.

[9] S. Yi, D. Labate, G. R. Easley, and H. Krim, *A Shearlet approach to Edge Analysis and Detection*, IEEE Trans. Image Process **18**(5) (2009), 929–941.

Construction and Applications of Shearlets

Wang-Q Lim

(joint work with Gitta Kutyniok, Jakob Lemvig)

It is now widely acknowledged that analyzing the intrinsic geometrical features of a function/signal is essential in many applications. In order to achieve this, several directional systems have been proposed in the past. The first breakthrough was achieved by Candés and Donoho who introduced curvelets and showed that curvelets provide an optimally sparse approximation property for a special class of 2D piecewise smooth functions, called cartoon-like images. Since then, various directional systems have been proposed. Recently, a novel directional representation system – so-called shearlets [7] – has emerged which provides a unified treatment of such continuum models as well as digital models, allowing, for instance, a precise resolution of wavefront sets, optimally sparse representations of cartoon-like images, and associated fast decomposition algorithms. Shearlet systems are systems generated by one single generator with parabolic scaling, shearing, and translation operators applied to it, in the same way wavelet systems are dyadic scalings and translations of a single function, but including a directionality characteristic owing to the additional shearing operation (and the anisotropic scaling). Further, in the series of papers [5, 6], we showed that it is possible to construct compactly supported shearlets systems and they provide an optimally sparse approximation property for larger classes of functions than a class of cartoon-like images. We now introduce a general approach to construct compactly supported shearlet systems.

We first start with some notations and definitions for later use. For $j \geq 0, k \in \mathbb{Z}$, let

$$A_{2^j} = \begin{pmatrix} 2^j & 0 \\ 0 & 2^{j/2} \end{pmatrix}, \ \tilde{A}_{2^j} = \begin{pmatrix} 2^{j/2} & 0 \\ 0 & 2^j \end{pmatrix} \quad \text{and} \quad S_k = \begin{pmatrix} 1 & k \\ 0 & 1 \end{pmatrix},$$

Next we define discrete shearlet systems in 2D. Let c be a positive constant. For $\phi, \psi, \tilde{\psi} \in L^2(\mathbb{R}^2)$ the *cone-adapted 2D discrete shearlet system* $SH(\phi, \psi, \tilde{\psi}; c)$ is defined by

$$SH(\phi, \psi, \tilde{\psi}; c) = \Phi(\phi; c) \cup \Psi(\psi; c) \cup \tilde{\Psi}(\tilde{\psi}; c), \tag{1}$$

where

$$\Phi(\phi; c) = \{\phi(\cdot - cm) : m \in \mathbb{Z}^2\},$$
$$\Psi(\psi; c) = \{2^{\frac{3}{4}j}\psi(S_k A_{2^j} \ \cdot \ -cm) : j \geq 0, -\lceil 2^{j/2}\rceil \leq k \leq \lceil 2^{j/2}\rceil, m \in \mathbb{Z}^2\},$$

and

$$\tilde{\Psi}(\tilde{\psi}; c) = \{2^{\frac{3}{4}j}\tilde{\psi}({S^T}_k \tilde{A}_{2^j} \ \cdot \ -cm) : j \geq 0, -\lceil 2^{j/2}\rceil \leq k \leq \lceil 2^{j/2}\rceil, m \in \mathbb{Z}^2\}.$$

We are now ready to state general sufficient conditions for the construction of shearlet frames.

Theorem 1 (Thm. 3.4 in [5]). *Let $\phi, \psi \in L^2(\mathbb{R}^2)$ be functions such that*

$$\hat{\phi}(\xi_1, \xi_2) \leq C_2 \cdot \min\{1, |\xi_1|^{-\gamma}\} \cdot \min\{1, |\xi_2|^{-\gamma}\}$$

and

$$|\hat{\psi}(\xi_1, \xi_2)| \leq C_1 \cdot \min\{1, |\xi_1|^{\alpha}\} \cdot \min\{1, |\xi_1|^{-\gamma}\} \cdot \min\{1, |\xi_2|^{-\gamma}\},$$

for some positive constants $C_1, C_2 < \infty$ and $\alpha > \gamma > 3$. Define $\tilde{\psi}(x_1, x_2) = \psi(x_2, x_1)$. Then there exits the sampling constant $c_0 > 0$ such that the shearlet system $SH(\phi, \psi, \tilde{\psi}; c)$, defined in (1), forms a frame for $L^2(\mathbb{R}^2)$ for all $c \leq c_0$ provided that there exits a positive constant $L > 0$ such that

$$|\hat{\phi}(\xi)|^2 + \sum_{j \geq 0} \sum_{k=-\lceil 2^{j/2}\rceil}^{\lceil 2^{j/2}\rceil} |\hat{\psi}({S^T}_k A_{2^j}\xi)|^2 + |\hat{\tilde{\psi}}((S_k)\tilde{A}_{2^j}\xi)|^2 > L$$

for a.e $\xi \in \mathbb{R}^2$.

In fact, one can construct compactly supported shearlet frames generated by a separable function, using Theorem 1. Further, this construction can be generalized to construct compactly supported 3D shearlets frames providing an optimally sparse approximation for a certain class of functions. We refer to [5, 6] for more details.

Shearlet theory has applications in various areas. we will now present two applications: Denoising of images and geometric separation of data. First, to illustrate how shearlets perform in image denoising, we have included a denoising example of the Goldhill image using both curvelets[1] and shearlets, see Figure 1. We omit

FIGURE 1. Denoising of the Goldhill image (512×512) using shearlets and curvelets. Left to Right : Original image, Noisy image (PSNR 20.17 dB), Curvelet-denoised image (PSNR 28.70 dB/ Computing time 7.22sec), Shearlet-denoised image (PSNR 29.20 dB / Computing time 5.56sec).

a detailed analysis of the denoising results and leave the visual comparison to the reader. For a detailed review of the shearlet transform and associated aspects, we refer to [8]. In neurobiological imaging, it is desirable to separate two morphologically different objects, namely 'dendrites' and 'spines', from neuron image in order to analyze them separately. The shearlet transform, in companion with a wavelet transform, has also been applied to accomplish geometric separation of 'point-and-curve'-like data. Especially, this separation scheme can be used to separate dendrites and spines from neuron image. The result of our geometric separation of neuron image can be seen in Figure 2. For a theoretical account of these separation ideas and implementation, we refer to [4, 1]. Designing a directional representation system that efficiently handles data with anisotropic features is quite challenging since it needs to satisfy a long list of desired properties: simple mathematical structure, optimally sparse approximations of certain image classes, compactly supported generators, fast decomposition algorithms, and unified treatment of the continuum and digital realm. We argue that shearlets meet all these challenges, and are, therefore, one of the most successful directional systems. However, the mathematical properties of dual frames for compactly supported shearlet frames are still unknown. Further, it is not known whether compactly supported tight shearlet frames exist. Our next tasks will include the mathematical analysis of

[1]Produced using Curvelab (Version 2.1.2), which is available from http://curvelet.org (also see [2]).

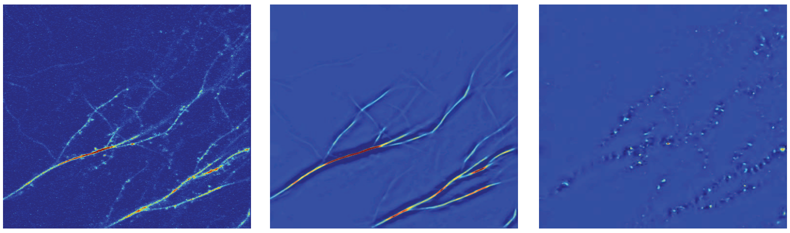

FIGURE 2. Left to Right : Noisy neuron image, Separated image (Dendrites 'curves'), Separated image (Spines 'points').

dual shearlet frames and the constructions of compactly supported tight shearlet frames – if they exist.

References

[1] R. Brandt, G. Kutyniok, W.-Q Lim, and F. Sündermann, *Extraction of dendrite and dendritic spines in neurobiological imaging*, in preparation.

[2] E. J. Candés, L. Demanet, D. Donoho, L. Ying, *Fast discrete curvelet transforms*, Multiscale Model. Simul. **5** (2006), 861–899.

[3] E. J. Candés and D. L. Donoho, *New tight frames of curvelets and optimal representations of objects with piecewise C^2 singularities*, Comm. Pure and Appl. Math. **56** (2004), 216–266.

[4] D. L. Donoho and G. Kutyniok, *Microlocal analysis of the geometric separation problem*, preprint.

[5] P. Kittipoom, G. Kutyniok, and W.-Q Lim, *Construction of compactly supported shearlet frames*, preprint.

[6] G. Kutyniok, J. Lemvig, and W.-Q Lim, *Compactly supported shearlet frames and optimally sparse approximations of functions in $L^2(\mathbb{R}^3)$ with piecewise C^2 singularities*, preprint.

[7] D. Labate, W.-Q Lim, G. Kutyniok, and G. Weiss. *Sparse multidimensional representation using shearlets*, Wavelets XI (San Diego, CA, 2005), 254–262, SPIE Proc. **5914**, SPIE, Bellingham, WA, 2005.

[8] W.-Q Lim, *The discrete shearlet transform: A new directional transform and compactly supported shearlet frames*, IEEE Trans. Image Proc. **19** (2010), 1166–1180.

Optimally Sparse Approximations of Functions in $L^2(\mathbb{R}^3)$ with C^α Singularities using Shearlets

Jakob Lemvig

(joint work with Gitta Kutyniok, Wang-Q Lim)

Many important problem classes are governed by anisotropic features such as singularities concentrated on lower dimensional embedded manifolds. To analyze the ability of representation systems to reliably capture and sparsely represent anisotropic structures, Donoho [1] introduced the model situation of so-called cartoon-like images, i.e., two-dimensional functions which are C^2 smooth apart from a C^2 discontinuity curve. In the past years, it was shown that curvelets, contourlets, and shearlets all have the ability to essentially optimal sparsely approximate cartoon-like images measured by the L_2-error of the (best) n-term approximation. Traditionally, this type of results has only been available for band-limited generators, but recently Kutyniok and Lim [2] showed that optimal sparsity also holds for spatial compactly supported shearlet generators under weak moment conditions.

In this report, we introduce generalized three-dimensional cartoon-like images, i.e., three-dimensional functions which are C^β except for discontinuities along C^α surfaces for $\alpha, \beta \in (1, 2]$, and consider sparse approximations of such. We first derive the optimal rate of approximation which is achievable by exploiting information theoretic arguments. Then we introduce three-dimensional pyramid-adapted shearlet systems with compactly supported generators and prove that such shearlet systems indeed deliver essentially optimal sparse approximations of three-dimensional cartoon-like images. Finally, we even extend this result to the situation of surfaces which are C^α except for zero- and one-dimensional singularities, and again derive essential optimal sparsity of the constructed shearlet frames.

We start by defining the 3D cartoon-like image class. Fix $\nu > 0$. By $\mathcal{E}_3^{2,2}(\nu)$ we denote the set of functions $f : \mathbb{R}^3 \to \mathbb{C}$ of the form

$$f = f_0 + f_1 \chi_B,$$

where $B \subset [0, 1]^3$ with ∂B a closed C^2-surface for which the principal curvatures are bounded by ν and $f_i \in C^2(\mathbb{R}^3)$ with $\mathrm{supp} f_i \subset [0, 1]^3$ and $||f_i||_{C^2} \leq 1$ for each $i = 0, 1$. We enlarge this cartoon-like image model class to allow less regular images as follows. Let $1 < \alpha, \beta \leq 2$. We then require that ∂B is, not necessarily a C^2-surface, but a C^α-surface, and that $f_i \in C^\beta(\mathbb{R}^3) \cap H^\beta(\mathbb{R}^3)$ with $||f_i||_{C^\beta} \leq 1$ for each $i = 0, 1$. We speak of $\mathcal{E}_3^{\alpha,\beta}(\nu)$ as consisting of generalized cartoon-like 3D images having C^β smoothness apart from a C^α discontinuity surface.

In [3], it was shown that the optimal approximation rate for such 3D cartoon-like image models $f \in \mathcal{E}_3^{\alpha,\beta}(\nu)$ which can be achieved for almost any representation system (under polynomial depth search selection procedure of the approximating coefficients) is

$$\|f - f_n\|_2^2 = O(n^{-\min\{\alpha/2, 2\beta/3\}}), \quad n \to \infty,$$

where f_n is the best n-term approximation of f. In the following paragraphs we introduce shearlet systems for $L^2(\mathbb{R}^3)$ which almost deliver this approximation rate.

The *Pyramid-Adapted Shearlet Systems* are defined as follows. We partition the frequency space into three pairs of pyramids:

$$\mathcal{P} = \{(\xi_1, \xi_2, \xi_3) \in \mathbb{R}^3 : |\xi_1| \geq 1,\ |\xi_2/\xi_1| \leq 1,\ |\xi_3/\xi_1| \leq 1\},$$
$$\tilde{\mathcal{P}} = \{(\xi_1, \xi_2, \xi_3) \in \mathbb{R}^3 : |\xi_2| \geq 1,\ |\xi_1/\xi_2| \leq 1,\ |\xi_3/\xi_2| \leq 1\},$$
$$\breve{\mathcal{P}} = \{(\xi_1, \xi_2, \xi_3) \in \mathbb{R}^3 : |\xi_3| \geq 1,\ |\xi_1/\xi_3| \leq 1,\ |\xi_2/\xi_3| \leq 1\},$$

and a centered rectangle:

$$\mathcal{R} = \{(\xi_1, \xi_2, \xi_3) \in \mathbb{R}^3 : ||(\xi_1, \xi_2, \xi_3)||_\infty < 1\}.$$

We first consider the shearlet system associated with the pyramid pair $\mathcal{P}$.

Fix $\alpha \in (1, 2]$. We scale according to the *scaling matrix* A_{2^j}, $j \in \mathbb{Z}$, and represent directionality by the *shear matrix* S_k, $k = (k_1, k_2) \in \mathbb{Z}^2$, defined by

$$A_{2^j} = \begin{pmatrix} 2^{j\alpha/2} & 0 & 0 \\ 0 & 2^{j/2} & 0 \\ 0 & 0 & 2^{j/2} \end{pmatrix}, \qquad S_k = \begin{pmatrix} 1 & k_1 & k_2 \\ 0 & 1 & 0 \\ 0 & 0 & 1 \end{pmatrix},$$

respectively. The case $\alpha = 2$ correspond to paraboloidal scaling; allowing $\alpha = 1$ would yield isotropic scaling. The translation lattices will be generated by the matrix $M_c = \mathrm{diag}(c_1, c_2, c_2)$, where $c_1 > 0$ and $c_2 > 0$. The shearlet system associated with $\mathcal{P}$ generated by $\psi \in L^2(\mathbb{R}^3)$ is defined as

$$\Psi(\psi; c) = \{2^{(1/2+\alpha/4)j}\psi(S_k A_{2^j} \cdot - m) \, : \, j \geq 0, |k_1|, |k_2| \leq \lceil 2^{(\alpha-1)j/2} \rceil, m \in M_c\mathbb{Z}^3\},$$

The shearlet systems associated with $\tilde{\mathcal{P}}$ and $\breve{\mathcal{P}}$ are defined in a similar manner (simply switch the role of the variables and append $\tilde{\cdot}$ and $\breve{\cdot}$, respectively, to suitable symbols).

The partition of the frequency space into pyramids allows us to restrict the range of the shear parameters. In the case of 'shearlet group' systems, one must allow arbitrarily large shear parameters, while the 'pyramid-adapted' systems restrict the shear parameters to $[-2^{(\alpha-1)j/2}, 2^{(\alpha-1)j/2}]$. It is exactly this fact that gives a more uniform treatment of the directionality properties of the shearlet system.

We are now ready to introduce our 3D shearlet system. For fixed $\alpha \in (1, 2]$ and $c = (c_1, c_2) \in (\mathbb{R}_+)^2$, the *pyramid-adapted 3D shearlet system* $SH(\phi, \psi, \tilde{\psi}, \breve{\psi}; c, \alpha)$ generated by $\phi, \psi, \tilde{\psi}, \breve{\psi} \in L^2(\mathbb{R}^3)$ is defined by

$$SH(\phi, \psi, \tilde{\psi}, \breve{\psi}; c) = \Phi(\phi; c_1) \cup \Psi(\psi; c, \alpha) \cup \tilde{\Psi}(\tilde{\psi}; c) \cup \breve{\Psi}(\breve{\psi}; c),$$

where

$$\Phi(\phi; c_1) = \{\phi(\cdot - m) \, : \, m \in c_1\mathbb{Z}^3\}.$$

The functions $\phi, \psi, \tilde{\psi}, \breve{\psi} \in L^2(\mathbb{R}^3)$ are called shearlets, and the function ϕ is a scaling function associated the centered rectangle $\mathcal{R}$.

In [3], it is shown that one can construct frames of the form $SH(\phi, \psi, \tilde{\psi}, \breve{\psi}; c, \alpha)$, where the generators $\phi, \psi, \tilde{\psi}, \breve{\psi} \in L^2(\mathbb{R}^3)$ are compactly supported. The following result tells us that compactly supported pyramid-adapted shearlets provide almost optimal approximation rate for the class of generalized 3D cartoon-like images.

Theorem 1 ([3]). *Let $\alpha \in (1, 2]$ and $c \in (\mathbb{R}_+)^2$, and let $\phi, \psi, \tilde{\psi}, \breve{\psi} \in L^2(\mathbb{R}^3)$ be compactly supported. Suppose that, for all $\xi = (\xi_1, \xi_2, \xi_3) \in \mathbb{R}^3$, the function ψ satisfies:*

(i) $|\hat{\psi}(\xi)| \leq C \cdot \min\{1, |\xi_1|^\delta\} \cdot \min\{1, |\xi_1|^{-\gamma}\} \cdot \min\{1, |\xi_2|^{-\gamma}\} \cdot \min\{1, |\xi_3|^{-\gamma}\}$,

(ii) $\left|\frac{\partial}{\partial \xi_i}\hat{\psi}(\xi)\right| \leq |h(\xi_1)| \cdot \left(1 + \frac{|\xi_2|}{|\xi_1|}\right)^{-\gamma} \cdot \left(1 + \frac{|\xi_3|}{|\xi_1|}\right)^{-\gamma}$, *for* $i = 1, 2$, *where* $\delta > 8$, $\gamma \geq 4$, $h \in L^1(\mathbb{R})$, *and* C *a constant, and suppose that* $\tilde{\psi}$ *and* $\breve{\psi}$ *satisfy analogous conditions with the obvious change of coordinates. Further, suppose that the shearlet system* $SH(\phi, \psi, \tilde{\psi}, \breve{\psi}; c, \alpha)$ *forms a frame for* $L^2(\mathbb{R}^3)$.

Then, for any $\beta \in (1, 2]$ *and* $\nu > 0$, *the frame* $SH(\phi, \psi, \tilde{\psi}, \breve{\psi}; c, \alpha)$ *provides almost optimally sparse approximations of functions* $f \in \mathcal{E}_3^{\alpha,\beta}(\nu)$ *in the sense that:*

$$\|f - f_n\|_2^2 = O(n^{-\min\{\alpha/2-\epsilon, 2\beta/3\}}) \qquad \text{as } n \to \infty,$$

where $\epsilon = \epsilon(\alpha)$ *satisfies* $\epsilon < 0.04$ *and* f_n *is the nonlinear* n*-term approximation obtained by choosing the* n *largest shearlet coefficients of* f.

For $\alpha = 2$, we even have $\|f - f_n\|_2^2 = O(n^{-\min\{\alpha/2, 2\beta/3\}} (\log n)^2)$ in Theorem 1 which is optimal (up to a log-factor). We remark that a large class of generators $\psi, \tilde{\psi}$, and $\breve{\psi}$ satisfy the conditions (i) and (ii) in Theorem 1. Theorem 1 is a three-dimensional version of a result from [2]. However, as opposed to the two-dimensional setting, anisotropic structures in three-dimensional data comprise of *two* morphologically different types of structure, namely surfaces *and* curves. It would therefore be desirable to allow our 3D image class to also contain cartoon-like images with *curve* singularities. To achieve this we allow our discontinuity surface ∂B to be a closed, continuous, *piecewise* C^α smooth surface. We denote this function class $\mathcal{E}_3^{\alpha,\beta}(\nu, L)$, where $L \in \mathbb{N}$ is the maximal number of C^α pieces. Surprisingly, the pyramid-adapted shearlet systems still deliver the same almost optimal rate for this extended image class $\mathcal{E}_3^{\alpha,\beta}(\nu, L)$. We refer to [3] for the precise statement of the result.

References

[1] D. L. Donoho, *Sparse components of images and optimal atomic decomposition*, Constr. Approx. **17** (2001), 353–382.

[2] G. Kutyniok and W.-Q Lim, *Compactly supported shearlets are optimally sparse*, preprint.

[3] G. Kutyniok, J. Lemvig, and W.-Q Lim, *Compactly supported shearlet frames and optimally sparse approximations of functions in* $L^2(\mathbb{R}^3)$ *with piecewise* C^α *singularities*, preprint.

An introduction to mocklets

Filippo De Mari

(joint work with Enesto De Vito)

The *mocklets* are the admissible vectors for a class of representations of suitable semi-direct products which generalize the metaplectic representation of the symplectic group as restricted to its (standard) parabolic subgroups. The setup is the following:

i) the Hilbert space of signals is $L^2(\mathbb{R}^d)$, regarded in the frequencies domain;
ii) the parameter space G is the semi-direct product $G = \mathbb{R}^n \rtimes H$, where H is a locally compact second countable group with an n-dimensional representation $h \mapsto M_h$ (hence M_h is an $n \times n$ matrix);

iii) the group H acts also on $\mathbb{R}^d$ by a C^∞ action $(h,x) \mapsto h.x$ in such a way that there exists a positive character β of H for which
$$\int_{\mathbb{R}^d} \varphi(h^{-1}.x) = \beta(h) \int_{\mathbb{R}^d} \varphi(x)dx \qquad \varphi \in C_c(X).$$
Thus, for $h \in H$ the Jacobian of the map $x \mapsto h.x$ does not depend on x;

iv) a C^∞ map $\Phi : \mathbb{R}^d \to \mathbb{R}^n$ such that, for all $x \in X$ and $h \in H$
$$\Phi(h.x) = h[\Phi(x)] = {}^tM_h^{-1}\Phi(x).$$

The *mock-metaplectic* representation is the representation that acts on $L^2(\mathbb{R}^d)$ as
$$(U_{(a,h)}f)(x) = \beta(h)^{-\frac{1}{2}} e^{-2\pi i\langle \Phi(x),a\rangle} f(h^{-1}.x).$$

Our results in [1] are based on the following two assumptions:

H1 the H-orbits in the dual group $\mathbb{R}^n$ are locally closed;

H2 for almost all $y \in \Phi(\mathbb{R}^d)$ the stability subgroup of y is compact.

The first result gives a necessary condition to have a reproducing formula: the "translations" group $\mathbb{R}^n$ needs to be smaller than the space where the signals are defined.

Theorem 1. *If U is a reproducing representation, then the set of critical points of Φ has zero Lebesgue measure, hence $n \leq d$.*

From now on we assume the existence of an open H-invariant subset $X \subset \mathbb{R}^d$ on which the Jacobian of Φ is strictly positive and whose complement is negligible. As a consequence, $Y = \Phi(X)$ is an H-invariant open set of $\mathbb{R}^n$ and each level set $\Phi^{-1}(y)$ is a Riemannian submanifold (with Riemannian measure dv_y). The coarea formula gives the following disintegration formula for the d-dimensional Lebesgue measure dx: there exists a family $\{\nu_y\}_{y\in Y}$ of Radon measures on X such that

a) for all $y \in Y$ the measure ν_y is concentrated on $\Phi^{-1}(y)$;

b) for all $\varphi \in C_c(X)$ $\displaystyle\int_X \varphi(x)d\nu_y(x) = \int_{\Phi^{-1}(y)} \varphi(x)\frac{dv_y(x)}{(J\Phi)(x)}$;

c) for all $\varphi \in C_c(X)$ $\displaystyle\int_X \varphi(x)dx = \int_Y \Big(\int_X \varphi(x)d\nu_y(x)\Big)dy.$

The next step is to label the H-orbits of Y. The natural choice of the quotient space Y/H with the quotient topology can give rise to pathological spaces. However, H1 implies that there exist a locally compact second countable space Z with a Radon measure dz, a Borel map $\pi : Y \to Z$ and a family of Radon measures $\{\tau_z\}_{z\in Z}$ on Y with the following properties:

a) $\pi(y) = \pi(y')$ if and only if y and y' belongs to the same orbit and there is a Borel map $z \mapsto o(z)$ from $\Phi(Z)$ to Y such that $\pi(o(z)) = z$, so that $\pi^{-1}(z) = H[o(z)]$;

b) for all $z \in Z$, τ_z is concentrated on $\pi^{-1}(z)$ and is a relatively invariant measure with character $|\det(M_h)|^{-1}$;

c) for all $\varphi \in C_c(Y)$ $\displaystyle\int_Y \varphi(x)dy = \int_Z \Big(\int_Y \varphi(x)d\tau_z(y)\Big)dz.$

For all $z \in \pi(Y)$, we think of $o(z)$ as the origin of the orbit $\pi^{-1}(z) = H[o(z)]$ and we denote by $H_z = H_{o(z)}$ the stability subgroup of $o(z)$ and by $\nu_z = \nu_{o(z)}$ the H_z-invariant measure on the level set $\Phi^{-1}(o(z))$, which is H_z-invariant. Furthermore we fix the Haar measure ds on H_z is such a way that Weil's formula holds true

$$\int_H \varphi(h)|\det(M_h)|^{-1}\, dh = \int_Y \Big(\int_{H_z} \varphi(h_y\, s) ds\Big) d\tau_z(u) \qquad \varphi \in C_c(H),$$

where $h_y \in H$ is such that $h_y[o(z)] = y$ for all $y \in H[o(z)]$. Define π^z be the quasi-regular representation of H_z acting on $L^2(X, \nu_{o(z)})$ by

$$(\pi^z_s f_{o(z)})(x) = f_{o(z)}(s^{-1}.x) \qquad \nu_y\text{-a.e. } x \in \Phi^{-1}(o(z)).$$

Assumption H2 ensures that, up the a negligible set, H_z is compact, so that π^z is completely reducible

$$\pi^z \simeq \bigoplus_{i\in I} m_i\, \pi^{z,i} \qquad L^2(X, \nu_{o(z)}) \simeq \bigoplus_{i\in I} m_i\, \mathbb{C}^{d_i^z}$$

where each $\pi^{z,i}$ is an irreducible representation of H_z acting on some $\mathbb{C}^{d_i^z}$ and the cardinal $m_i \in \mathbb{N} \cup \{\aleph_0\}$ is the multiplicity of $\pi^{z,i}$ into π^z. It is possible to choose the index set I in such a way that m_i is independent of z (it can happen that $d_i^z = 0$).

We are now ready to characterize the existence of admissible vectors for the representation U, namely for the existence of mocklets.

Theorem 2. *Suppose that the set of critical points of Φ is negligible and Assumptions $H1$ and $H2$ hold true. If G is non-unimodular, then U is reproducing whereas if G is unimodular, U is reproducing if and only if*

$$\int_Z \frac{\operatorname{card}\Phi^{-1}(o(z))}{\operatorname{vol}(H_z)}\, dz < +\infty \qquad \textit{where } \operatorname{vol} H_z = \int_{H_z} ds$$
$$m_i \leq \dim(L^2(Y, \tau_z, \mathbb{C}^{d_{i,z}})) \qquad \forall i \in I\ ,\ \textit{almost every } z \in Z.$$

In [1] an explicit characterization of the admissible vectors is given.

An example. One of the main motivations for our construction is the connection with the continuous shearlet transform that we now illustrate. The full shearlet group $\mathbb{R}^2 \rtimes (\mathbb{R} \rtimes \mathbb{R}_+)$, with scaling γ, can be realized as a subgroup of the symplectic group $Sp(2, \mathbb{R})$ as follows. Fix $\gamma \in \mathbb{R}$ (in the usual shearlet literature we have $\gamma = 1/2$) and define

$$\sigma_t = \begin{bmatrix} t_1 & t_2 \\ t_2 & 0 \end{bmatrix}, \qquad M_s = \begin{bmatrix} 1 & 0 \\ -s & 1 \end{bmatrix}, \qquad M_a = \begin{bmatrix} a^{-1/2} & 0 \\ 0 & a^{1/2-\gamma} \end{bmatrix},$$

where $t = (t_1, t_2) \in \mathbb{R}^2$, $s \in \mathbb{R}$ and $a \in \mathbb{R}_+$. The matrices

$$g(a, s, t) = \begin{bmatrix} M_s M_a & 0 \\ \sigma_t M_s M_a & {}^t(M_s M_a)^{-1} \end{bmatrix}$$

form a subgroup G of $Sp(2, \mathbb{R})$ which is isomorphic to the shearlet group. It falls in the setup described above as follows. First of all, $H = \{M_s M_a\}$ and $n = d = 2$.

On the one hand $\mathbb{R}^2 = \mathbb{R}^d$ must be interpreted as frequency space (and its points are denoted by ω), and on the other hand $\mathbb{R}^2 = \mathbb{R}^n$ is the dual of the representation space of H (and its points are denoted by y). The H action on the frequency space $\mathbb{R}^2$ is $h.\omega = M_s M_a \omega$, whereas the contragredient representation is

$$h[y] = \begin{bmatrix} a^{-1} & 0 \\ -sa^{-1} & a^{-\gamma} \end{bmatrix} \begin{bmatrix} y_1 \\ y_2 \end{bmatrix}$$

The intertwining map is $\Phi(\omega_1, \omega_2) = -\frac{1}{2}(\omega_1^2, \omega_1\omega_2)$. It maps both half planes $X_L = \{\omega \in \mathbb{R}^2 : \omega_1 < 0\}$ and $X_R = \{\omega \in \mathbb{R}^2 : \omega_1 > 0\}$ onto X_L. By means of the restriction $\Phi_L = \Phi|_{X_L}$ we define the map $\Psi : L^2(X_L) \to L^2(X_L)$ by

$$\Psi f(y) = |J_{\Phi_L^{-1}}(y)|^{1/2} f(\Phi_L^{-1}(y)).$$

The inverse Fourier transform $\mathcal{F}^{-1}$ maps $L^2(X_L)$ onto a closed proper subspace $\mathcal{S} \subset L^2(\mathbb{R}^2)$ and it is easy to see that for $F \in \mathcal{S}$ we have

$$S_{a,s,t}\, F(\omega) = \mathcal{F}^{-1}\left(\Psi U_{g(a,s,t)} \Psi^{-1} \mathcal{F} F\right)(\omega),$$

where

$$S_{a,s,t} F(\omega) = a^{-3/4} F\left(\begin{bmatrix} a^{-1} & -sa^{-1} \\ 0 & a^{-\gamma} \end{bmatrix} \begin{bmatrix} \omega_1 - t_1 \\ \omega_2 - t_2 \end{bmatrix}\right)$$

is the continuous shearlet representation (see e.g. [2]) and where

$$U_{g(a,s,t)} f(\omega) = a^{\gamma/2} e^{i\pi\langle\sigma_t \omega, \omega\rangle} f\Big(\begin{bmatrix} a^{1/2} & 0 \\ sa^{\gamma-1/2} & a^{\gamma-1/2} \end{bmatrix} \omega\Big).$$

is the restriction of the metaplectic representation to G. All the hypotheses that we have introduced are easily satisfied. By applying our results one obviously finds the well-known conditions on admissible vectors, that is, on shearlets.

References

[1] F. De Mari and E. De Vito. *A mock metaplectic representation*, Technical report 589, DIMA, Università di Genova, (2010), http://www.dima.unige.it/ricerca/pubblicazioni.php.

[2] S. Dahlke, G. Kutyniok,G. Steidl and G. Teschke, *Shearlet Coorbit Spaces and Associated Banach Frames* , Applied and Computational Harmonic Analysis **27** (2009), 195-214.

Shearlet Multiresolution and Adaptive Directional Multiresolution

Tomas Sauer

(joint work with Gitta Kutyniok, Angelika Kurtz)

Like with the wavelet transform there are several ways and conceptional concepts to develop numerical implementations of the shearlet transform. The first, maybe more straightforward concept, is to sample the continuous transformation at a finite set of parameters chosen such that the resulting discrete transformation (hopefully) captures all information of the underlying transformed functions. In both cases, the numerical computation can be accelerated by using a Fast Fourier Transform to evaluate the underlying convolutions, cf[1]. The second approach, on the other hand, is entirely discrete and relies on filter banks and the concept of *multiresolution analysis* introduced by Mallat. The main ingredient for a multiresolution analysis, that is, a nested sequence $V_0 \subset V_1 \subset \cdots$ of spaces generated by translates of a finite set of functions, is the so–called *refinement equation* that relates the different dilation levels. In the simplest case of pure isotropic scaling, the refinement equation takes the form

$$\phi = \sum_{\alpha \in \mathbb{Z}^s} a(\alpha)\, \phi\,(2 \cdot -\alpha)$$

and any solution for such a functional equation with given *mask* a (usually a finitely supported function on $\mathbb{Z}^s$). Based on this property of the function ϕ and an appropriate interpretation of the discrete data c as coefficients of a *detail level representation*

$$\phi * c\,(2^n \cdot) = \sum_{\alpha \in \mathbb{Z}^s} \phi\,(2^n \cdot -\alpha)\; c(\alpha)$$

of a function in V_n, *dyadic* wavelet decompositions of this function can be computed entirely by means of filter banks. To mimic that approach for the shearlet approach, the two matrices

$$\Xi_0 = \begin{bmatrix} 4 & 0 \\ 0 & 2 \end{bmatrix}, \qquad \Xi_1 = \begin{bmatrix} 4 & -4 \\ 0 & 2 \end{bmatrix} = \Xi_0 \begin{bmatrix} 1 & -1 \\ 0 & 1 \end{bmatrix},$$

one being an anisotropic dilation, the other one that dilation combined with a simple shear, and two masks a_η, $\eta \in \{0,1\}$, are used in a interleaving fashion. Indeed, to any infinite sequence $\eta \in \{0,1\}^\infty$, one can assign a sequence of *subdivision schemes*

$$S_\eta^r c := S_{\eta_r} \cdots S_{\eta_1} c, \qquad S_\epsilon c = \sum_{\alpha \in \mathbb{Z}^s} a_\epsilon\,(\cdot - \Xi_\epsilon \alpha)\; c(\alpha), \quad \epsilon \in \{0,1\},$$

that converges, under suitable assumptions, for any η to a *limit function* f_η when applied to the δ–sequence that is 1 at the origin and vanishes on $\mathbb{Z}^s \setminus \{0\}$.

This family of limit functions shears with a slope related to the dyadic number $.\eta_1\eta_2\ldots$ and satisfies the *joint refinement equation*

$$f_{\epsilon,\eta} = \sum_{\alpha \in \mathbb{Z}^s} a_\epsilon(\alpha)\, f_\eta\,(\Xi_\epsilon \cdot -\alpha)\,, \qquad \epsilon \in \{0,1\},\, \eta \in \{0,1\}^\infty,$$

where the *refinement process* is determined by the first digit of the index and the *refining function* by the remaining infinite part of the index. Based on these functions, a multiresolution analysis can be built where, however, V_0 is generated by the integer translates of the countable set of all functions of the form $f_{(\eta,0,\ldots)}$ with finite initial index η. The talk was describing this construction from [2] and some numerical aspects, like complexity of the algorithm and some first results of a simple interpolatory multiresolution analysis implemented in [3].

References

[1] G. Kutyniok and T. Sauer. *From wavelets to shearlets and back again*, In L. L. Schumaker (ed.), *Approximation Theory XII (San Antonio, TX, 2007)*, 201–209. Nashboro Press, Nashville, 2008.

[2] G. Kutyniok and T. Sauer. *Adaptive directional subdivision schemes and shearlet multiresolution analysis*, SIAM J. Math. Anal, **41** (2009), 1436–1471.
[3] A. Kurtz, *Shearlet Multiresolution*, BA Thesis, JLU Gießen, 2010.

Image Processing Applications using Shearlets

Glenn R. Easley
(joint work with F. Colonna, H. Krim, D. Labate, S. Yi)

The shearlet representation has recently been shown to be much more effective than the traditional wavelet representation in dealing with the set of discontinuities of functions and distributions. In particular, shearlets have the ability to provide a very precise geometrical characterization of general discontinuity curves occurring in images. A formulation of the total variation method using shearlets for denoising images is proposed. It is also shown that the multiscale directional properties of shearlets can be used to design an algorithms for analysis and detection of edges. A general total variation (TV) technique for the purpose of denoising is commonly based on minimizing the functional

$$\int_\Omega \phi(\|\nabla u\|)\, dx\, dy + \frac{\lambda}{2}\int_\Omega (u-u_0)^2\, dx\, dy,$$

where $\phi \in C^2(\mathbb{R})$ is an even regularization function, λ is a fidelity parameter, and u and u_0 represent the estimate and noisy image, respectively. The solution is obtained by finding the steady state solution of

$$\frac{\partial u}{\partial t} = \nabla \cdot \left(\frac{\phi'(\|\nabla u\|)}{\|\nabla u\|}\nabla u\right) - \lambda(u-u_0)$$

subjected to the Neumann boundary condition. An improved performance of the general TV method can be achieved by incorporating a discrete shearlet transform as follows.

Given an appropriate generating function ψ, the discrete shearlets are the elements of the collection

$$\{\psi_{j,\ell,k} = |\det A|^{j/2}\, \psi(B^\ell A^j x - k) : j, \ell \in \mathbb{Z}, k \in \mathbb{Z}^2\},$$

where

$$B = \begin{pmatrix} 1 & 1 \\ 0 & 1 \end{pmatrix}, \quad A = \begin{pmatrix} a & 0 \\ 0 & \sqrt{a} \end{pmatrix},$$

with $a \in \mathbb{R}^+$. The discrete shearlets have the reproducing formula:

$$f = \sum_{j,\ell \in \mathbb{Z}, k \in \mathbb{Z}^2} \langle f, \psi_{j,\ell,k}\rangle\, \psi_{j,\ell,k}.$$

with convergence in the L^2 sense. Thus $f \in L^2(\mathbb{R}^2)$ can be very well approximated using a shearlet representation $\tilde{f}$ as

$$\sum_{j,\ell,k \in M_1} \langle f, \psi_{j,\ell,k}\rangle \psi_{j,\ell,k} + \sum_{j,\ell,k \in M_2} \langle f, \psi_{j,\ell,k}\rangle \psi_{j,\ell,k}$$

where the index sets M_1 and M_2 correspond to the coarse scale coefficients associated with the smooth regions of f and to the fine scale coefficients associated with the edges of f.

Denote by M_2^C the set of indices of M_2 in the shearlet domain that correspond to the coefficients that would be set to zero in the above reconstruction when estimating a denoised version. A projection operator P_S onto the reconstruction from these coefficients is defined as

$$P_S(u) = \sum_{j,\ell,k \in M_2^C} \langle u, \psi_{j,\ell,k} \rangle \psi_{j,\ell,k}.$$

Then the proposed method is to find the steady state solution of

$$\frac{\partial u}{\partial t} = \nabla \cdot \left(\tfrac{\phi'(\|\nabla P_S(u)\|)}{\|\nabla P_S(u)\|} \nabla P_S(u) \right) - \lambda_{x,y}(u - u_0)$$

with the boundary condition $\frac{\partial u}{\partial n} = 0$ on $\partial\Omega$ and the initial condition $u(x, y, 0) = u_0(x, y)$ for $x, y \in \Omega$, where Ω is the ambient space. Note that the quantity $\lambda_{x,y}$ is to be a spatially varying fidelity term based on a measure of local variances.

The shearlet transform's geometrical properties are also useful for edge analysis and for edge detection. The continuous shearlet transform can be expressed as

$$S_\psi u(a, s, x) = \int u(y)\, \psi_{as}(x - y)\, dy = u * \psi_{as}(x).$$

where the analyzing elements ψ_{as} are well localized waveforms at various scales and orientations. An edge detector is constructed using the following properties. If $u \in E^{1,3}(\Omega)$ (see [2] for details of this function space) and t is away from the edges, then $S_\psi u(a, s, t)$ decays rapidly as $a \to 0$, and the decay rate depends on the local regularity of u. In particular, if u is Lipschitz–α near $t_0 \in \mathbb{R}^2$, then the following estimates hold: for $\alpha \geq 0$,

$$|S_\psi u(a, s, t_0)| \leq C\, a^{\frac{1}{2}(\alpha + \frac{3}{2})}, \quad \text{as } a \to 0;$$

while for $\alpha < 0$,

$$|S_\psi u(a, s, t_0)| \leq C\, a^{(\alpha + \frac{3}{4})}, \quad \text{as } a \to 0.$$

Classification of points by their Lipschitz regularity is important and is used to distinguish true edge points from points corresponding to noise.

References

[1] G. R. Easley, D. Labate, and W. Lim, *Sparse Directional Image Representations using the Discrete Shearlet Transform*, Appl. Comput. Harmon. Anal., **25** (2008), 25–46.

[2] G. R. Easley, D. Labate, and F. Colonna, *Shearlet-Based Total Variation for Denoising*, IEEE Trans. Image Processing, **18**(2) (2009), 260–268.

[3] G. R. Easley, K. Guo, and D. Labate, *Analysis of Singularities and Edge Detection using the Shearlet Transform*, Proc. SAMPTA'09, Marseille, May 2009.

[4] K. Guo, D. Labate and W. Lim, *Edge Analysis and identification using the Continuous Shearlet Transform*, Appl. Comput. Harmon. Anal., **27**(1) (2009), 24–46.

[5] S. Yi, D. Labate, G. R. Easley, and H. Krim, *A Shearlet Approach to Edge Analysis and Detection*, IEEE Trans. Image Process. **18** (5) (2009), 929–941.

Image Restoration and Enhancement using Shearlets

Vishal M. Patel
(joint work with Glenn R. Easley, Dennis M. Healy, Jr.)

Shearlets provide a multi-directional and multi-scale decomposition that has been mathematically shown to represent distributed discontinuities such as edges better than traditional wavelets. We present several image processing applications such as image enhancement, image deconvolution and inverse halftoning using a shift-invariant overcomplete shearlet representation.

The first application deals with the problem of image enhancement in which the objective is to make the processed image better in some sense than the unprocessed image. Since edges contain important information about the image, they can be used to enhance the contrast. To this end, we develop a new nonlinear mapping function that modifies the shearlet coefficients such that it enhances weak edges and suppresses noise. Experimental results show that this enhancement technique achieves better results than wavelet-based enhancement methods.

In image restoration, the goal is to best estimate an image that has been degraded. Examples of image degradation include the blurring introduced by camera motion as well as the noise introduced from the electronics of the system. In the case when the degradations can be modelled as a convolution operation, the process of recovering the original image from the degraded blurred image is commonly called deconvolution. The process of deconvolution is known to be an ill-posed problem. Thus, to get a reasonable image estimate, a method of controlling noise needs to be utilized.

We propose a shearlet-based deconvolution algorithm which utilizes the power of a Fourier representation to approximately invert the convolution operator and a redundant shearlet representation to provide an image estimate. The multi-scale and multi-directional aspects of the shearlet transform provide a better estimation capability over that of the wavelet transform or wavelet-like transforms for images exhibiting piecewise smooth edges. In addition, we adapt a method of automatically determining the threshold values for the shearlet noise shrinkage without knowing the noise variance by using a generalized cross validation function. Various experiments show that this method can perform better than many the state-of-the-art wavelet-based deconvolution methods.

References

[1] V. M. Patel, G. R. Easley and D. M. Healy, Jr., *Shearlet-Based Deconvolution*, IEEE Transactions on Image Processing, **18** (2009), 2673–2685.

[2] V. M. Patel, G. R. Easley, and D. M. Healy, Jr., *A new multiresolution generalized directional filter bank design and application in image enhancement*, Proceedings of IEEE International Conference on Image Processing, (2008).

[3] V. M. Patel, G. R. Easley, and R. Chellappa, *Multiscale directional filtering of noisy InSAR phase images*, Defense, Security and Sensing, Proceedings of SPIE, (2010).

[4] G. R. Easley, V. M. Patel, and D. M. Healy, Jr., *Inverse halftoning using a shearlet representation*, Wavelets XIII, Proceedings of SPIE, (2009).

[5] G. R. Easley, V. Patel, and D. M. Healy, Jr., *An M-channel directional filter bank compatible with the contourlet and shearlet frequency tiling*, in Wavelets XII, Proceedings of SPIE, (2007).

The structure tensor and its relatives

Gabriele Steidl
(joint work with Tanja Teuber, Simon Setzer)

The classical structure tensor of Förstner and Gülch [3] is defined as follows: Assume that an image u is has nearly constant values along a direction r, $\|r\|_2 = 1$ in a neighborhood $B_\rho(x_0)$ of x_0 so that

$$0 \approx \frac{\partial}{\partial r} u(x) = r^{\mathrm{T}} \nabla f(x), \qquad x \in B_\rho(x_0).$$

Let w be a nonnegative weight function with support in $B_\rho(0)$. Then the relation

$$0 \approx \int\limits_{\Omega} w(x-x_0)\,(r^{\mathrm{T}}\nabla u(x))^2\,dx \;=\; r^{\mathrm{T}} \underbrace{\int\limits_{\Omega} w(x-x_0)\,\nabla u(x) \nabla u^{\mathrm{T}}(x)\,dx}_{J_w(\nabla u)(x_0)}\; r$$

holds true and consequently r is eigenvector of the smallest eigenvalue of $J_w(\nabla f)(x_0)$ For the Gaussian weight $w := K_\rho$ we get the *structure tensor*

$$J_\rho(\nabla u_\sigma) \;:=\; K_\rho * (\nabla u_\sigma \nabla u_\sigma^{\mathrm{T}}) \;=\; \underbrace{(r^\perp,\; r)}_{R} \begin{pmatrix} \mu_1 & 0 \\ 0 & \mu_2 \end{pmatrix} R^{\mathrm{T}}.$$

The structure tensor has various applications, e.g., in the diffusion tensor D which steer the flux in the anisotropic diffusion

$$\begin{aligned} \partial_t u &= \operatorname{div}\left(D(\nabla u_\sigma)\, \nabla u \right) \\ u(0,\cdot) &= f \\ \left(D(\nabla u_\sigma) \nabla u \right)^{\mathrm{T}} n &= 0, \end{aligned}$$

see, e.g., [9]. Anisotropic diffusion is closely related to variational approaches via the Euler-Lagrange equation. Consider the functional

$$E(u) = \frac{1}{2}\,\|f-u\|_{L_2}^2 \;+\; \lambda \int_\Omega \varphi(\nabla u(x))\,dx$$

with a positive, convex, positively-homogeneous function $\varphi : \mathbb{R}^2 \to \mathbb{R}$. Let $W_\varphi := \{y \in \mathbb{R}^2 : \langle y, x\rangle \le \varphi(x)\ \forall x \in \mathbb{R}^2\}$ denotes the *Wulff shape* of φ. If $f := 1_{W_\varphi}$, then for λ smaller than some constant the minimizer of E is given by $u = c\,1_{W_\varphi}$ for some $c > 0$, see [2]. Moreover there exist relations between anisotropic diffusion and Haar wavelet shrinkage which can be found in [8, 4, 10].

However, the classical structure tensor cannot find the directions at corners and X-junctions and is moreover not useful in the presence of impulse noise. Therefore we suggest to use the more general structure tensor of Aach et al. [1]. Using this structure tensor one can find the two directions r_1 and r_2 at corners (occlusion model) or X-junctions (transparent model). Then we apply the occlusion structure tensor to preserve sharp corners within the variational setting

$$E(u) = \frac{1}{2}\|f-u\|_2^2 + \lambda\|V(x)^{\mathrm{T}}\nabla u(x)\|_1 = \frac{1}{2}\|f-u\|_2^2 + \lambda(\|r_1^{\mathrm{T}}\nabla u\|_1 + \|r_2^{\mathrm{T}}\nabla u\|_1)$$

and the transparent structure tensor to get sharp X junctions within the *infimal-convolution regularization* setting

$$E(u) = \frac{1}{2}\|f-u\|_{L_2}^2 + \lambda \inf_{u_1+u_2=u} \int_\Omega |\langle r_1, \nabla u_1(x)\rangle| + |\langle r_2, \nabla u_2(x)\rangle|\, dx.$$

This leads to very good denoising and segmentation results, see [7, 6].

Finally, we replace the classical structure tensor which can also be written as *matrix mean*

$$\begin{aligned} \mathcal{J}_\rho(i_0,j_0) &= \frac{\sum\limits_{(i,j)\in\mathcal{N}(i_0,j_0)} w_{i_0-i,j_0-j}P_{i,j}}{\sum\limits_{(i,j)\in\mathcal{N}(i_0,j_0)} w_{i_0-i,j_0-j}} \\ &= \operatorname{argmin}_{X\in\mathbb{R}^{2,2}} \sum_{(i,j)\in\mathcal{N}(i_0,j_0)} w_{i_0-i,j_0-j}\|X-P_{i,j}\|_{\mathcal{F}}^2 \end{aligned}$$

by special *matrix medians*

$$X(i_0,j_0) := \operatorname{argmin}_{X\in\mathbb{R}^{2,2}} \sum_{(i,j)\in\mathcal{N}(i_0,j_0)} w_{i_0-i,j_0-j}\|X-P_{i,j}\|_\bullet$$

where $\|\cdot\|_\bullet$ stands for a unitarily invariant matrix norm. Here we restrict our attention to the nuclear norm, the Frobenuis norm and the spectral norm. We show how to find a minimizer of this functional by various numerical methods as the alternating direction method of multipliers, the parallel proximal algorithm, the primal-dual hybrid gradient method and second order cone programming. Moreover, we discuss relations between these matrix medians and Euclidian vector medians based on the isometry $T : \mathrm{Sym}_2(\mathbb{R}) \to \mathbb{R}^3$ given by

$$T(X) := \frac{1}{\sqrt{2}}(x_{1,1} - x_{2,2}, 2x_{1,2}, x_{1,1} - x_{2,2})^{\mathrm{T}}.$$

For the involved vector medians it appears that the Weiszfeld algorithm performs well. Finally, we present numerical results. This last part of the talk is based on [5].

References

[1] T. Aach, C. Mota, I. Stuke, M. Mühlich, and E. Barth. Analysis of superimposed oriented patterns. 15(12):3690–3700, 2006.

[2] S. Esedoglu and S. J. Osher. Decomposition of images by the anisotropic Rudin-Osher-Fatemi model. *Communications in Pure and Applied Mathematics*, 57(12):1609–1626, 2004.

[3] W. Förstner and E. Gülch. A fast operator for detection and precise location of distinct points, corners and centres of circular features. In *Proc. ISPRS Intercommission Conference on Fast Processing of Photogrammetric Data*, pages 281–305, Interlaken, Switzerland, June 1987.

[4] P. Mrazek, J. Weickert, and G. Steidl. Diffusion-inspired shrinkage functions and stability results for wavelet shrinkage. *International Journal of Computer Vision*, 64(2/3):171 – 186, 2005.
[5] S. Setzer, G. Steidl, and T. Teuber. On vector and matrix computation. *Preprint Univ. Mannheim*, 2010.
[6] G. Steidl and T. Teuber. Anisotropic smoothing using double orientations. volume 5567 of *LNCS*, pages 477–489. Springer, 2009.
[7] G. Steidl and T. Teuber. Diffusion tensors for denoising sheared and rotated rectangles. *IEEE Trans. Image Processing*, 18(12):2640 – 2648, 2009.
[8] G. Steidl, J. Weickert, T. Brox, P. Mrazek, and M. Welk. On the equivalence of soft wavelet shrinkage, total variation diffusion, total variation regularization, and sides. *SIAM J. Numer. Anal.*, 42(2):686 – 658, 2004.
[9] J. Weickert. *Anisotropic Diffusion in Image Processing*. Teubner, Stuttgart, 1998.
[10] M. Welk, G. Steidl, and J. Weickert. Locally analytic schemes: a link between diffusion filtering and wavelet shrinkage. *Applied and Computational Harmonic Analysis*, (24):195 – 224, 2008.

Interpolating Refinable Function Vectors and Matrix Extension with Symmetry

Xiaosheng Zhuang
(joint work with Bin Han)

A function (vector) $\phi = [\phi_1, \cdots, \phi_r]^T : \mathbb{R} \mapsto \mathbb{C}^{r\times 1}$ is d-*refinable* if

$$\phi = \mathsf{d} \sum_{k\in\mathbb{Z}} a(k)\phi(\mathsf{d}\cdot -k).$$

Refinable functions play an important role in both theory and application. On the one hand, functions composed from linear combinations of shifts of a refinable function ϕ can be computed using a simple subdivision scheme, which makes subdivision curves and surfaces very attractive for interactive geometric modeling applications. On the other hand, it allows for the definition of a nested sequences of shift-invariant spaces. This so-called "multiresolution analysis (MRA)" is the key to wavelet constructions. It has been realized that the most desired properties of wavelets are orthogonality, symmetry, interpolation, compact support, regularity and so on. These properties usually conflict to each other. With "MRA", the design of wavelets with desired properties is significantly reduced to the design of a d-*refinable function (vector)* with certain properties. Once ϕ is obtained, the wavelets (multiwavelets, framelets) can be derived under some "Extension Principle" (unitary extension principle, oblique extension principle).

Among many subdivision schemes, interpolatory subdivision schemes and Hermite interpolatory subdivision schemes are of great interest in sampling theory, numerical algorithms, computer graphics and so on. For example, wavelets constructed by means of an interpolating refinable function provide a nice Shannon-like sampling theorem which proved to be useful in signal processing. In image processing, orthogonal wavelets are often used in denoising and compression. And it is known that the Daubechies orthogonal wavelets can be obtained from interpolatory masks via Rieze lemma. Also, functions with interpolation property have been intensively studied and play an fundamental roles in approximation theory.

While orthogonality and interpolation property are important in applications, there is no compact 2-refinable function that is both interpolating and orthogonal. In order to achieve both interpolation and orthogonality, in which case, the coefficients in the multiresolution representatition can be realized by *sampling* instead of inner product, it is necessary to consider either d-refinable functions with $\mathsf{d} > 2$ or refinable function vectors. Our work is related to the later one which allows us to construct mutliwavelets that are both interpolating and orthogonal. Here is a summary of our work on this subject (see [1, 2]):

(1) We introduce a new notation of *interpolating* d*-refinable function vectors of type* (r, h), which includes both the definitions of refinable interpolants and refinable Hermite interpolants. An interpolating d-refinable function vectors of type (r, h) is a d-refinable function vector that interpolates on the lattice $r^{-1}\mathbb{Z}$ up to Hermite order h.
(2) Provide a complete mathematical characterization for such interpolating d-refinable function vectors of type (r, h) in terms of their masks and derive the sum rule structure of such interpolatory masks explicitly, which are crucial in the construction of interpolating d-refinable function vector of type (r, h).
(3) Construct a family of d-refinable function vectors of type (r, h) with arbitrary orders of sum rules in 1D. Provide examples with properties of orthogonality, interpolation and symmetry.
(4) Provide a characterization of such interpolating refinable function vectors in any dimension to be symmetry with respect to a general symmetry group (D_4, D_6 for example) in terms of their masks. Construct several examples of interpolating refinable function vectors in 2D that are symmetry with respect to symmetry groups D_4, D_6.

As mentioned, once ϕ is obtained, the construction of wavelets from ϕ is reduced to a extension problem. For the construction of orthogonal multiwavelets, the problem is: "Let P be an $n \times r$ matrix of Laurent polynomials with $\mathsf{P}^*\mathsf{P} = I_r$. How to extend it to a square $(n \times n)$ unitary(paraunitary) matrix $\mathsf{A} = [\mathsf{P}\ \mathsf{Q}]$." Here, P is constructed from the polyphase representation of the mask a for ϕ. Even without considering any symmetry issue, as far as we know, there are no results for general $r \geq 1$ showing that the support of the extension matrix is controlled by the original P. When comes to symmetry, things get much more complicated. The difficulties lie in "extension with symmetry" and "support control of the extension matrix". Yet both symmetry and small support of wavelet systems are important and sometimes crucial in wavelet applications. Even if we leave aside double reduction of the computational costs of symmetric system, the "Linear Phase" property, which significantly reduces visual artifacts in image processing, can not be compensated by any other properties. We solve this problem completely under the symmetry setting. Here is a summary (see [3]):

(1) Under a natural symmetry condition on P, we prove that P can be extended to a unitary matrix A such that A has certain symmetry pattern closely related to that of P, the support of A is controlled by that of P in a subtle way, i.e., the support control is column-wised, and A can be represented as a serial of low degree unitary matrices (a cascade structure in engineering).
(2) We develop a simple step-by-step algorithm producing the extension unitary matrix A such that A has certain symmetry pattern, its support is controlled by the support of P and A is represented by a serial of low degree unitary matrices.
(3) Matrix extension plays an important role in many areas of electronic engineering, system sciences, applied mathematics, as well as pure mathematics. As a application of our general result on matrix extension with symmetry, we obtain a satisfactory algorithm for constructing high-pass filters with symmetry from given low-pass filters in paraunitary multiwavelet filter banks.
(4) Unlike most known results working only on $\mathbb{R}$ or $\mathbb{C}$, our work is under a general field $\mathbb{F}$, which can be any subfield of $\mathbb{C}$ that is closed under square root and complex conjugate.

References

[1] B. Han, S. G. Kwon and X. Zhuang, Generalized interpolating refinable function vectors, *Journal of Computational and Applied Mathematics*, **227** (2009), 254-270.
[2] B. Han and X. Zhuang, *Analysis and construction of multivariate interpolating refinable function vectors*, Acta Applicandae Mathematicae, **107** (2009), No. 1-3, 143-171.
[3] B. Han and X. Zhuang, *Matrix extension with symmetry and its application to symmetric otrhonormal multiwavelets*, SIAM Journal on Mathematical Analysis, **42** (2010), 2297–2317.

Reporter: Demetrio Labate

Participants

Prof. Dr. Bernhard G. Bodmann
Department of Mathematics
University of Houston
Houston TX 77204-3008
USA

Prof. Dr. Stephan Dahlke
FB Mathematik & Informatik
Philipps-Universität Marburg
Hans-Meerwein-Strasse (Lahnbg.)
35032 Marburg

Prof. Dr. Filippo De Mari
DIPTEM
Universita di Genova
P'le Kennedy, Pad. D
I-16129 Genova

Prof. Dr. Ernesto De Vito
Dipartimento di Matematica
Universita di Genova
Via Dodecaneso 35
I-16146 Genova

Dr. Glenn R. Easley
System Planning Corporation
100 Wilson Boulevard
Arlington , VA 22209-2211
USA

Dr. Philipp Grohs
Seminar for Applied Mathematics
ETH-Zentrum
Rämistr. 101
CH-8092 Zürich

Prof. Dr. Kanghui Guo
Department of Mathematics
Missouri State University
901 South National Ave.
Springfield, MO 65897
USA

Prof. Dr. Gitta Kutyniok
FB Mathematik/Informatik
Universität Osnabrück
Albrechtstr. 28a
49076 Osnabrück

Prof. Dr. Demetrio Labate
Department of Mathematics
University of Houston
Houston TX 77204-3008
USA

Dr. Jakob Lemvig
FB Mathematik/Informatik
Universität Osnabrück
Albrechtstr. 28a
49076 Osnabrück

Dr. Wang-Q. Lim
FB Mathematik/Informatik
Universität Osnabrück
Albrechtstr. 28a
49076 Osnabrück

Dr. Vishal Patel
Center for Automation Research
University of Maryland
A.V. Williams Bldg.
College Park , MD 20742
USA

Prof. Dr. Tomas Sauer
Lehrstuhl für Numerische Mathematik
Universität Gießen
Heinrich-Buff-Ring 44
35392 Giessen

Prof. Dr. Gabriele Steidl
Fak. für Mathematik u. Informatik
Universität Mannheim
D 7, 27
68131 Mannheim

Prof. Dr. Gerd Teschke
Hochschule Neubrandenburg
University of Applied Sciences
Brodaer Straße 2
17033 Neubrandenburg

Dr. Xiaosheng Zhuang
Department of Mathematical and
Statistical Sciences
University of Alberta
632 Central Academic Building
Edmonton, Alberta T6G 2G1
CANADA